

# Spectro Biogas

**Online measurement of process parameters for better process understanding- control and performance at Danish biogas plants.**

**Danish Technological Institute**

**August 2023**

**Parisa Ghofrani-Isfahani, DTU**

**Irini Angelidaki, DTU**

**Kurt Hjort-Gregersen, DTI**

## Table of contents

1. Background
2. Challenges
3. Abstract for pilot testing at DTU
4. Trials with SPECTRO sensor at DTU
5. Effect of sulfur compounds in anaerobic digestion performance
6. Test and validation of the SPECTRO sensor
7. Use of SPECTRO sensor for gas-liquid mass transfer parameter determination.
8. Operation of the reactor equipped with SPECTRO sensor for anaerobic digestion process
9. Conclusion of the DTU tests
10. General discussion and economic perspectives

## 1. Background

The company Spectro Biogas developed a sensor for online measurement of process parameters in biogas digesters as well as other biological processes. The technology is based on mass spectroscopy.

The technology is already to some extent applied on digesters in sewage sludge treatment facilities. The overall objective of this project was to gain knowledge and experience for the application of the sensor system on agricultural biogas plants. Not only to test the ability of the system to monitor crucial process parameters of the biogas process, but also to interpret the measured data into a control system, to enable plant operators to utilize the data for process monitoring and to take specific actions according to signals from the system.

As a part of the project, Spectro Biogas had the system tested at Sønderjysk Biogas. The test was foreseen to take place during the last part of the project, but for commercial reasons Spectro Biogas chose to carry out the tests somewhat sooner in the project. However, for commercial reasons, Spectro Biogas has preferred to publish results from the full-scale testing as a part of the official reporting of this project. Consequently, this report mainly contains results from the comprehensive testing of the sensor at DTU.

Partners in the project were Spectro Biogas A/S, Danish Technical University, Department of Chemical and Biochemical Engineering (DTU) and Danish Technological Institute (DTI).

Project management was taken care of by DTI.

The project was supported by EUDP. The project period ranged from 1<sup>st</sup> June 2020 to 31<sup>st</sup> Juli 2023.

Contact information of authors

Parisa Ghofrani-Isfahani, DTU [parisf@kt.dtu.dk](mailto:parisf@kt.dtu.dk)

Irini Angelidaki, DTU, [iria@kt.dtu.dk](mailto:iria@kt.dtu.dk)

Kurt Hjort-Gregersen, DTI, [kuhj@teknologisk.dk](mailto:kuhj@teknologisk.dk)

## 2. Challenges.

- a. As Spectro Biogas decided to test the sensor full scale at Sønderjysk Biogas meant that it could not be installed at DTU as foreseen. It was agreed that a new sensor, which was being constructed at the time, would be installed at DTU as soon as possible. However, during the full scale testing it turned out problematic that the sensor was quite sensitive to pulsating pump flows, which in fact caused the sensor chip to break, causing liquids to flow into the sensor compromising electrical components etc., which had then to be repaired. These issues caused several delays in the project time schedule.
- b. Spectro Biogas is a small company with limited staff resources, and at least one key staff member left for another job during the project period, which most likely is one of the reasons for some of the delays.
- c. When the sensor finally arrived at DTU it had to be combined with the DTU digester set-up. It is a digester enabled for continuous operation, very suitable for the tests. However, additional spare parts were needed, especially as it turned out that the connection between digester and sensor was leaking, which is an untenable situation to have in a laboratory, especially when we talk about cattle manure. This problem led to further delay.
- d. After the system was up and running at DTU the final missing issue was the data link from the sensor to Spectro Biogas. As a university, DTU has comprehensive protection of their internal network, and it turned out to be more than difficult to be allowed to establish a direct data link to an external partner. Finally, the solution was establishing a mobile connection fully independent of the DTU internal network. This delay set the DTU testing under severe time pressure, and the project was granted a further prolongation until 31st July 2023.
- e. It is well known that the key parameters for biogas process monitoring are the volatile fatty acids (VFAs). And it was anticipated by Spectro Biogas (and the project manager) that the sensor was able to measure the fatty acids in agricultural biogas plants, because the system does that on digesters at sewage treatment plants. However, due to high ratios of animal manure in agricultural biogas plants in Denmark, Ph levels are most often relatively high compared to sewage sludge digesters, namely often Ph 7 or more. At such high Ph levels, the sensor is not able to measure VFAs. This of course, is a serious disadvantage for the use of the sensor on agricultural biogas plants. However, Spectro Biogas had reason to believe that if further developed it might be able to do so in the future, but further efforts need to be taken.

On the other hand, the sensor can measure a number of other dissolved gasses in the liquid phase of the digesters, of which a few are quite important and worth monitoring. More on that in the discussion.

### **3. Abstract for pilot testing at DTU.**

The project report evaluates the performance of the SPECTRO sensor, which is based on mass-spectroscopy for online monitoring of biogas production process. The sensor's accuracy in detecting concentration of dissolved gases such as CH<sub>4</sub>, CO<sub>2</sub>, H<sub>2</sub>, and N<sub>2</sub>, both individually and in mixtures, was assessed against measurement from gas chromatography analyses. The sensor demonstrated the ability to monitor gas concentrations in the liquid phase. However, the accuracy was medium, and measurement required re-calibration. Although the SPECTRO sensor could measure the dissolved gases concentrations in the liquid phase, these measurements were not adequately reliable indicators for process monitoring and control especially for manure-based biogas digesters with high buffer capacity. The VFAs concentration together with methane production rate would be ideal state indicators for process monitoring, control and early detection of process imbalance. The sensor was tested within an anaerobic digester fed with cattle manure for biogas production process. The sensor was not capable to measure VFAs concentrations and therefore the digester operated without designed control strategy based on VFAs concentrations and methane production rate. Therefore, it was concluded that titrimetric methods could be the most appropriate method for online VFAs measurements in anaerobic digestion process (AD). A control strategy based on online VFAs concentrations and methane production is a promising direction for future biogas process monitoring and control.

## **4. Trials with SPECTRO sensor at DTU**

### **4.1. Online monitoring and control of anaerobic digestion process**

Successful biogas production requires proper monitoring and control to improve the process efficiency and keep the process stable. The growing number of industrial biogas plants has led to the development of more advanced monitoring and control systems to keep the process stable. Furthermore, controlling the biological processes specially in complex systems, e.g. AD processes, is a very hard task since these processes are highly non-linear and their kinetic parameters are usually uncertain (Petre et al., 2013). Biogas plants often suffer from overload or inhibition due to change of feedstock and they are usually run under sub-optimal condition to avoid process instability. Therefore, utilizing proper controller is necessary to prevent biogas plants from failure. During the last years, various variables such as pH, alkalinity, volatile fatty acids (VFAs) concentrations or biogas production rate have been used for online monitoring, and several control strategies have been proposed for controlling anaerobic digesters (Jimenez et al., 2015; Petre et al., 2013; Steyer et al., 1999). In industrial biogas plants, biogas production rate is commonly used as process indicator since it represents the overall process performance and can be easily measured by many robust online sensors (Nguyen et al., 2015). Moreover, pH and titrimetric VFA estimation are applied in several biogas plants, although these values are not actively involved in process control. Taking biogas production as the only process state indicator is in many cases inadequate and can lead to under-loading since it does not take into account the health of the biogas process. For example, the biogas production rate starts to decrease when the process is already damaged (Boe et al., 2010). Thus, monitoring of biogas production rate is not enough for early detection of process imbalance to prevent failure in the bioreactor and other indicators are needed to be monitored simultaneously (Boe et al., 2010). Biogas production rate and pH are often the online measurements monitored in industrial biogas plants. However, for systems with higher buffer capacity, such as those treating manures, pH becomes less sensitive to process imbalances. The most promising parameter for predicting process imbalance is the concentration of specific VFAs, which are formed as intermediates during the anaerobic conversion process (Boe & Angelidaki, 2006). Therefore, VFAs concentration can be used as a suitable controlled variable (Ahring et al., 1995; Jacobi et al., 2009; Molina et al., 2009). Currently, VFA analysis can be performed by manual sample preparation and measurement by gas chromatographic or HPLC analysis. However, the procedure is time and labor consuming, requires expert personnel, and is expensive. The on-line application of mentioned techniques is limited due to poor sample preparation, filtration

and clogging issues. Thus, on-line monitoring of VFAs concentration has become a fundamental challenge in monitoring of AD process, therefore over the last few years, spectroscopic techniques have gained interest within the biotechnology field. This project aims to develop a novel spectrometry-based sensor as a fast, reliable and low maintenance on-line measurement device for on-line VFAs monitoring which would be able to predict biogas process upsets as early warning for preventing process break downs. Therefore, a novel control strategy is designed by utilizing methane production rate, VFAs and pH as online measured variables to optimize biogas production process.

## 4.2 Control strategy

The aim of control system is to improve methane production rate, while keeping the reactor stable in the presence of unexpected disturbances. In this project, a supervisory control strategy has been proposed to improve the methane production rate in an anaerobic digestion process while minimizing the risk of process failure. Feed flow rate was chosen as the manipulated variable in the control strategy, which was controlled by manipulating the feeding time with the same concentration. The supervisory control structure consisted of two loops, inner and outer loops where individual VFAs concentration (Acetic acid + Propionic acid, Ac\_Pr), pH and methane production rate were the measured variables. The inner loop was a feedback control loop using a proportional-Integral controller (PI) that manipulated the feed flow rate (FF) to achieve methane production rate set-point. A rule-based control was applied in the outer loop that used the methane flow rate (GF) trend and acetic acid and propionic concentrations (VFAs) in the reactor to provide the set-point of the inner control loop. Methanogenesis takes place in a pH range about 6.5 to 8.5 (Weiland, 2010). Therefore, an inter-lock system was considered based on the pH measurement in the reactor to prevent the system from acidification. If pH fell below 6, the FF was set to zero for the next feeding cycle. Otherwise, the supervisory controller remained active. The summation of acetic acid and propionic acid concentrations and methane production rate measurements were used at the supervisory level to select the appropriate rule in the rule-based control, thus updating the set-point of the inner loop. The proportional gain and integral time of the PI controller,  $K_c$  and  $\tau_i$  were calculated based on the data derived from a step change in feed flow rate reported in previous research (Boe et al., 2010) using the Internal Model Control (IMC) technique (*Process Dynamics and Control - Dale E. Seborg, Thomas F. Edgar, Duncan A. Mellichamp, Francis J. Doyle, III - Google Books, n.d.*). The control algorithm was programmed in LabVIEW2016 software (National Instruments, Austin, TX, USA) to change the manipulated variable (i.e. feed flow rate) based

on the control strategy described above. The rules applied in supervisory control are presented in Table 1:

### Nomenclature and notations used in control strategy

FF	Feed flow rate
GF	Gas (methane) flow rate
GF <sub>s.p.</sub>	Methane flow rate set-point
GF(t)	Methane production per 6 hours (mL/6 hours)
GF <sub>s.p.</sub> (t)	Current set-point value of methane production
GF <sub>s.p.</sub> (t-1)	Set-point value of methane production in previous cycle
GF <sub>step</sub>	Step change
GF <sub>min</sub> (t)	Minimum gas set-point value at time t
FF(t)	Current feed flow rate
FF(t-1)	Feed flow rate in previous cycle
Ac_Pr(t)	Summation of acetic and propionic acid concentration in current time
Ac_Pr(t-1)	Acetic and propionic acid concentration in previous cycle
pH(t)	Current pH value from the measurements

Table 1. The rule-based control strategy

Rule No.	Conditions	Set-point adjustment	Control action
1	if $GF(t) \geq GF_{\text{set point}}(t-1)$	$GF_{\text{set point}}(t) = GF_{\text{set point}}(t-1) + GF_{\text{step}}$	if $e(t) > 0$ $FF(t)^* = FF(t)$ otherwise $FF(t) = FF(t-1)$
2	if $GF_{\text{min}}(t-1) \leq GF(t) < GF_{\text{set point}}(t-1)$	$GF_{\text{set point}}(t) = GF_{\text{set point}}(t-1) + 0.5 \times GF_{\text{step}}$	$FF(t) = FF(t)$
3	if $GF(t) < GF_{\text{min}}(t-1)$ and previously at state 1	$GF_{\text{set point}}(t) = GF_{\text{set point}}(t-1)$	$FF(t) = \min[FF(t-1), FF(t)]$

4	if $GF(t) < GF_{\min}(t-1)$ and previously not at state 1 and $1.5 \leq Ac_{Pr}(t) < 3$ g/L and $Ac_{Pr}(t) - Ac_{Pr}(t-1) \leq Ac_{Pr}(t-1)$	$GF_{\text{set point}}(t) = GF_{\text{set point}}(t-1) - 0.5 GF_{\text{step}}$	$FF(t) = \min[FF(t-1), FF(t)]$
5	if $GF(t) < GF_{\min}(t-1)$ and previously not at state 1 and $1.5 \leq Ac_{Pr}(t) < 3$ g/L and $Ac_{Pr}(t-1) < Ac_{Pr}(t) - Ac_{Pr}(t-1) < 2 * Ac_{Pr}(t-1)$	$GF_{\text{set point}}(t) = GF_{\text{set point}}(t-1) - GF_{\text{step}}$	$FF(t) = \min[FF(t-1), FF(t)]$
6	if $GF(t) < GF_{\min}(t-1)$ and previously not at state 1 and $1.5 \leq Ac_{Pr}(t) < 3$ g/L and $2 * Ac_{Pr}(t-1) \leq Ac_{Pr}(t) - Ac_{Pr}(t-1)$	$GF_{\text{set point}}(t) = GF_{\text{set point}}(t-1) - 2 * GF_{\text{step}}$	$FF(t) = \min[FF(t-1), FF(t)]$
7	if $GF(t) < GF_{\min}(t-1)$ and previously not at state 1 and $3 \leq Ac_{Pr}(t) < 5$ g/L and $Ac_{Pr}(t) - Ac_{Pr}(t-1) < Ac_{Pr}(t-1)$	$GF_{\text{set point}}(t) = GF_{\text{set point}}(t-1) - GF_{\text{step}}$	$FF(t) = \min[FF(t-1), FF(t)]$
8	if $GF(t) < GF_{\min}(t-1)$ and previously not at state 1 and $3 \leq Ac_{Pr}(t) < 5$ g/L and $Ac_{Pr}(t-1) \leq Ac_{Pr}(t) - Ac_{Pr}(t-1)$	$GF_{\text{set point}}(t) = GF_{\text{set point}}(t-1) - 2 * GF_{\text{step}}$	$FF(t) = \min[FF(t-1), FF(t)]$
9	if $GF(t) < GF_{\min}(t-1)$ and previously not at state 1 and $5 \leq Ac_{Pr}(t)$ g/L	$GF_{\text{set point}}(t) = GF_{\text{set point}}(t-1) - 2 * GF_{\text{step}}$	$FF(t) = \min[FF(t-1), FF(t)]$
10	if $GF(t) < GF_{\min}(t-1)$ and previously at one of states of 4 to 9 and $Ac_{Pr}(t) < 1.5$ g/L	$GF_{\text{set point}}(t) = GF_{\text{set point}}(t-1)$	$FF(t) = \min[FF(t-1), FF(t)]$
11	if $GF(t) < GF_{\min}(t-1)$ and previously not at state 1 and none of states 4 to 9 and $Ac_{Pr} < 1.5$ g/L and $Ac_{Pr}(t) \geq Ac_{Pr}(t-1)$	$GF_{\text{set point}}(t) = GF_{\text{set point}}(t-1)$	$FF(t) = \min[FF(t-1), FF(t)]$
12	if $GF(t) < GF_{\min}(t-1)$ and previously not at state 1 and none of states 4 to 9 and $Ac_{Pr}(t) < 1.5$ g/L and $Ac_{Pr}(t) < Ac_{Pr}(t-1)$	$GF_{\text{set point}}(t) = GF_{\text{set point}}(t-1) + 0.5 GF_{\text{step}}$	$FF(t) = \max[FF(t-1), FF(t)]$
13	if $FF(t) = FF_{\max}$ $FF_{\max}$ : is the maximum allowable feed flow rate to prevent wash out	$GF_{\text{set point}}(t) = GF_{\text{set point}}(t-1)$	$FF(t) = FF_{\max}$

As the SPECTRO sensor could measure a number of dissolved gas compounds ( $CH_4$ ,  $CO_2$ ,  $H_2$ ,  $N_2$ ,  $NH_3$  and  $H_2S$ ) and VFAs which are relevant for biogas production optimization, 2 different scenarios were considered to use the sensor output for optimum process monitoring;

- 1) A control strategy was designed and developed based on methane production rate and pH monitored by on-line sensors and VFAs concentrations measured by SPECTRO sensor.
- 2) Different batch and continuous experiments were conducted to essay the effect of sulfur compounds on biogas production process as dissolved H<sub>2</sub>S can be detected by SPECTRO sensor.

## **5. Effect of sulfur compounds in anaerobic digestion performance:**

The overall aim was to investigate the effect of H<sub>2</sub>S (a variable also measured easily and reliably by the Spectro Biogas sensor) on the AD process and define its optimal range for stable operation. Later during the continuous reactor operation with the SPECTRO sensor, H<sub>2</sub>S concentration in the liquid phase would be monitored online which should be within the acceptable boundaries (H<sub>2</sub>S <300 ppm).

In this section, the effect of different sulfur compounds including sulfate and sulfide (SO<sub>4</sub><sup>2-</sup> and S<sup>2-</sup>) on anaerobic digestion process is studied through different batch and continuous lab-scale experiments.

### **5.1 Introduction on effect of sulfur compounds in biogas production process:**

Anaerobic digestion of high sulfur content feedstocks such as seaweed, pig manure, wastewater sludge and etc. (Peu et al., 2012) is a big challenge in biogas plants since sulfur suppress the process productivity and cause more H<sub>2</sub>S production in output gas. Existence of sulfur compounds in feedstocks causes methanogens inhibition leading to lower methane production and high amount of H<sub>2</sub>S in output biogas which is highly toxic and corrosive. Sulfur is usually present in the form of either sulfate or sulfides; however, other intermediates also exist such as sulfur dioxide, hydrogen sulfite, and thiosulfite. Sulfate is reduced to sulfides by sulfate reducing bacteria (SRBs) during AD. SRBs compete with methanogens and acetogens for their common nutritional needs (acetate, propionate, butyrate, formate, lactate and hydrogen) results in inhibition of AD process and decrease in methane production (Lackner et al., 2020). Optimization of sulfur type and its content in biogas plant feedstock could be an effective approach to shift the microbial community from SRBs to methanogens and increase the methane production while keeping H<sub>2</sub>S content at minimum level which is extremely important specially from economic and environmental points of view. For this purpose, different forms of sulfur compounds were added to feedstock to study the mechanisms, performance, and their impacts on pathways involved in AD process. By investigating the microbial community of

inhibitory or stimulatory mechanisms in presence of different sulfur compounds, it is possible to improve process efficiency and methane productivity during AD process.

## 5.2 Results and discussion on sulfur experiments:

### 5.2.1 Batch-scale anaerobic digestion experiments:

Effect of sulfate ( $\text{SO}_4^{2-}$ ) and ( $\text{S}^{2-}$ ) on AD was investigated by adding four different concentration levels (0.2 g S/L, 0.4 g S/L, 0.8 g S/L, and 1.6 g S/L) of either  $\text{Na}_2\text{SO}_4$  or  $\text{Na}_2\text{S}$  to batch reactors with cattle manure. The total and working volume in the batch reactors were 250 and 100 mL, respectively. A gas phase analysis, as well as a liquid phase analysis of the batch reactors were carried out. The gas phase analysis was performed using two Thermo Scientific Trace 1310 gas chromatograph (GC) to measure biogas composition ( $\text{CH}_4$ ,  $\text{CO}_2$ ,  $\text{H}_2$ ,  $\text{N}_2$  and  $\text{H}_2\text{S}$ ) in the reactor's headspace. The batch reactors were divided into blank reactors containing inoculum, control reactors containing inoculum and substrate (cattle manure), and main reactors which contained cattle manure, inoculum, and salts ( $\text{Na}_2\text{SO}_4$  and  $\text{Na}_2\text{S}$ ). Furthermore, the inoculum was degassed in a  $55^\circ\text{C}$  incubator prior to use. The reactors were flushed for ~5 minutes with  $\text{N}_2$  to create anaerobic conditions. They were then sealed with aluminum caps over rubber stoppers. The batch reactors were stored in a  $55^\circ\text{C}$  incubator for the duration of the experiment.

The characteristics of the inoculum and substrate (cattle manure) are shown in Table 2.

Table 2. The characteristics of the inoculum and substrate (cattle manure)

	Cattle manure	Inoculum
pH	7.67	8.1
TS, %	2.53 $\pm$ 0.02	2.74 $\pm$ 0.05
VS, %	2.0 $\pm$ 0.02	1.67 $\pm$ 0.02
Ash, %	0.53 $\pm$ 0.004	0.59 $\pm$ 0.02
TKN, g $\text{kg}^{-1}$	0.93 $\pm$ 0.0009	4.79 $\pm$ 0.31
TAN, g $\text{kg}^{-1}$	0.5 $\pm$ 0.003	4.61 $\pm$ 0.18
$\text{SO}_4^{2-}$ , mg $\text{L}^{-1}$	<0.5	<0.5
S (solid), mg $\text{kg}^{-1}$	3077.8 $\pm$ 615.56	8664.2 $\pm$ 363.9
S (liquid), mg $\text{L}^{-1}$	7.0 $\pm$ 0.23	19.6 $\pm$ 0.31
Total VFA, mmol $\text{L}^{-1}$	10.07 $\pm$ 0.78	3.45 $\pm$ 0.05
Acetate, mmol $\text{L}^{-1}$	7.74 $\pm$ 0.75	3.21 $\pm$ 0.05
Propionate, mmol $\text{L}^{-1}$	1.77 $\pm$ 0.18	0.14 $\pm$ 0.005
Iso-butyrate, mmol $\text{L}^{-1}$	0.13 $\pm$ 0.01	-
Butyrate, mmol $\text{L}^{-1}$	0.16 $\pm$ 0.01	0.08 $\pm$ 0.001
Iso-valerate, mmol $\text{L}^{-1}$	0.2 $\pm$ 0.01	-
Valerate, mmol $\text{L}^{-1}$	0.04 $\pm$ 0.001	-
Hexanoate, mmol $\text{L}^{-1}$	-	-

### 5.2.1.1 Batch results with Na<sub>2</sub>SO<sub>4</sub> addition:

As it is shown in Figure 1, all levels of Na<sub>2</sub>SO<sub>4</sub> had lower production of CH<sub>4</sub> compared to the control. Level 1 had decreased the least with a 77% decrease of CH<sub>4</sub> yield compared to the control. Level 2, 3 and 4 had decreased the CH<sub>4</sub> yield by 82%, 83% and 86%, compared to the control, respectively. Thus, the methanogenesis inhibition increased by increasing concentrations of Na<sub>2</sub>SO<sub>4</sub> in the batch reactors.

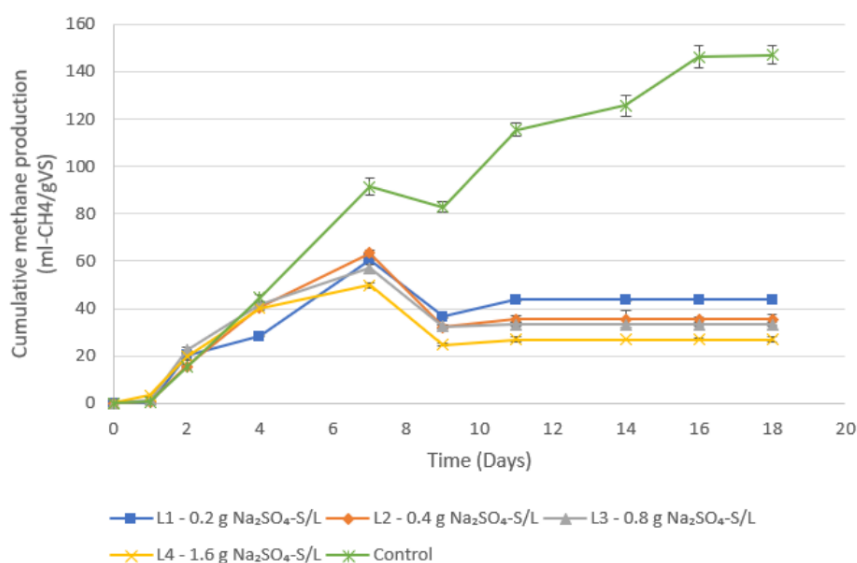


Figure 1 CH<sub>4</sub> production over time for four different levels of Na<sub>2</sub>SO<sub>4</sub> and control. On day 7 the measurement was performed on a different GC due to maintenance which could be why the values are relatively high. The batch reactors were in duplicates.

The total VFAs concentration in the liquid shown in Figure 2 shows that most of the VFAs had been consumed by day 7. At this point the reactors containing Na<sub>2</sub>SO<sub>4</sub> had already started to show decreased levels of CH<sub>4</sub> production. However, the total VFAs concentration started to increase after day 7 for level 1 and on day 28 the concentration was 5.9 mmol/L. The vast majority of the total VFAs was acetic acid, while some propionic acid was also present, as well as small fractions of other acids such as butyric acid. One possibility for the accumulation of VFA that was observed for level 1 is incomplete oxidation by SRBs (Chen et al., 2008). These types of SRBs use substrate such as propionate, lactate, ethanol, and methanol and produce acetate which was the most abundant VFA on day 14 and 28 for level 1. The pH results were shown in Figure S1 and S2 in Appendix.

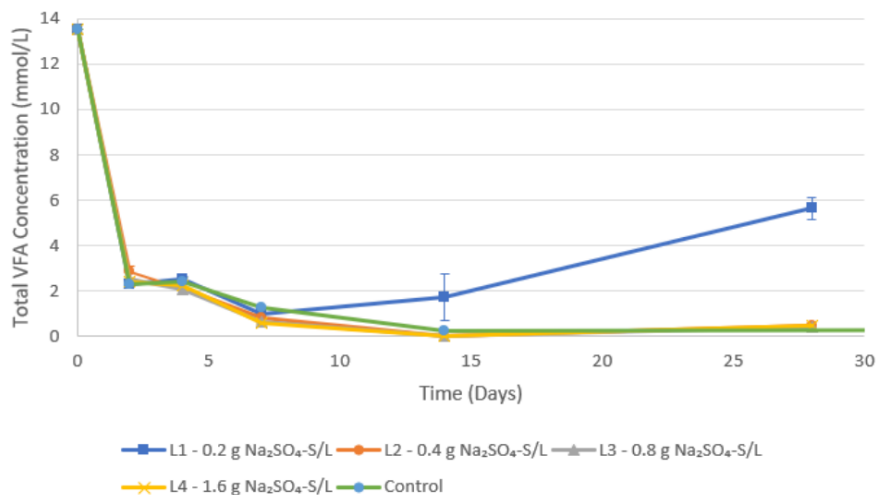


Figure 2 Concentration of total VFAs (mmol/L) over time for each concentration level and control in the liquid phase. The initial total VFAs concentration at  $t=0$  was 13.5 mmol/L. The VFAs analysis was carried out in duplicates.

Furthermore, the competition for substrate was the main factor for decreased CH<sub>4</sub> yield.

It should be mentioned that, during the gas phase analysis, both H<sub>2</sub>S and H<sub>2</sub> were measured with the GC. However, the concentrations of H<sub>2</sub>S were all below detection limit, and the H<sub>2</sub> concentrations measured for the entire duration were 0.01-0.02% which would put it within detection error range. The H<sub>2</sub>S and H<sub>2</sub> measurement results are therefore not included here.

### 5.2.1.2 Batch results with Na<sub>2</sub>S addition:

Analysis of the batch reactors with Na<sub>2</sub>S showed that level 1 had (0.2 g S/L) increased the final yields of CH<sub>4</sub> by 18% compared to the control, see Figure 3. Level 2 (0.4 g S/L) had the same CH<sub>4</sub> yield as the control, while level 3 and level 4 (0.8 and 1.6 g S/L, respectively) had decreased the CH<sub>4</sub> yield by 15% and 25%, respectively. However, as the experiment was stopped after 49 days, it is unclear whether the reported final yields for level 3 and 4 were in fact the final yields due to not reaching steady state.

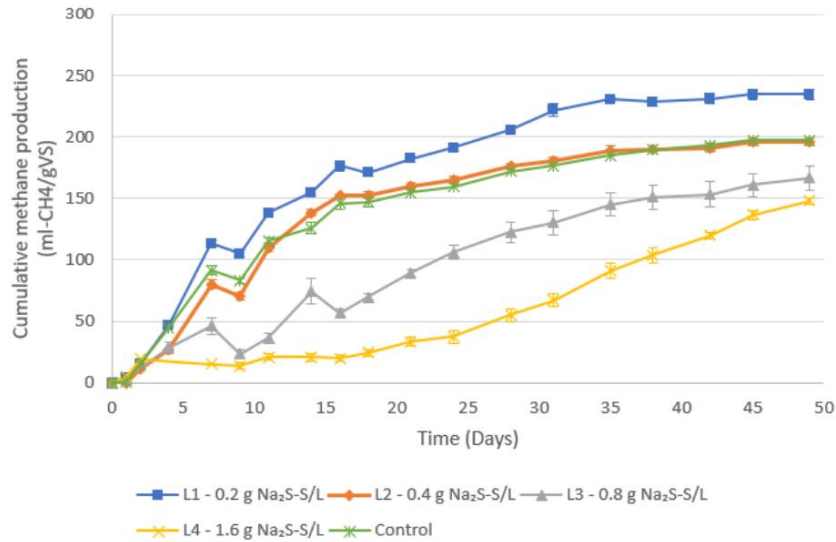


Figure 3 CH<sub>4</sub> production over time at four different levels of Na<sub>2</sub>S and control. The experiment was made with duplicates. On day 7 the measurement was performed on a different GC due to maintenance which could be why the values are relatively high. The batch reactors were in duplicates.

The total VFAs concentration analysis showed that level 1 followed a trend very similar to the control (see Figure 4). The total VFAs in level 1 was not fully consumed on day 2 and by day 4 the concentration had increased a small amount. However, the VFAs concentration started to decrease after day 4 and by day 14 all of the VFAs had been consumed by methanogens. Level 2 on the other hand, increased in terms of VFAs concentration after day 2 but by day 7, the VFAs started to decrease. VFAs in level 3 was fully consumed initially, however, after day 4 the VFA started to accumulate for the remainder of the duration. VFA in level 4, on the other hand, decreased from its initial point and by day 7, the concentrations started to accumulate for the remainder of the duration. The majority of the total VFA concentration was acetic acid, and to a lesser degree propionic acid. No other VFAs were detected.

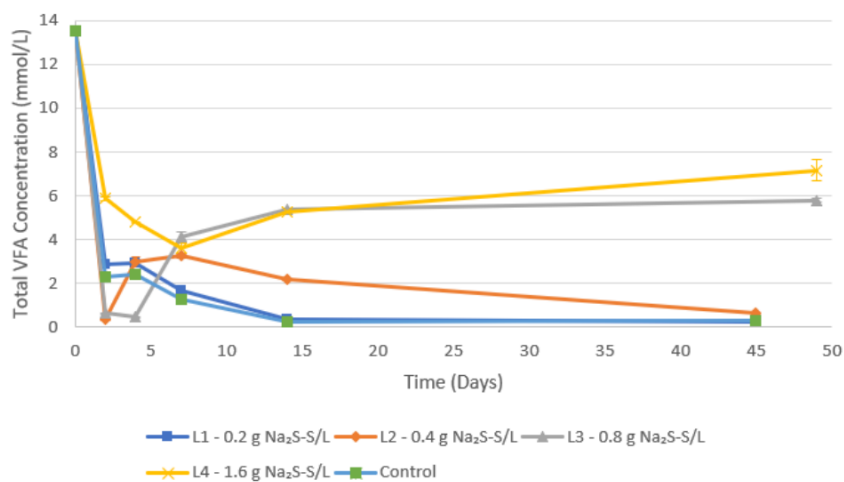


Figure 4 Concentration of total VFA in the liquid phase (mmol/L) for batch reactors with Na<sub>2</sub>S added over.

Therefore, as a conclusion, the addition of  $\text{SO}_4^{2-}$  in all levels cause severe inhibition of the  $\text{CH}_4$  production from AD. On the other hand, when  $\text{Na}_2\text{S}$  was used for the batch reactors, level 1 (0.2 g  $\text{Na}_2\text{S}$ -S/L) had increased the yield of  $\text{CH}_4$  by 18% compared to the control, while level 2 had similar yield as the control, and the  $\text{CH}_4$  yield in level 3 and 4 was lower than the control. This was likely caused by a longer lag phase caused by high initial concentrations of sulfide from the  $\text{Na}_2\text{S}$ .

It was unclear why the  $\text{CH}_4$  yield increased by 18% when the concentration of  $\text{Na}_2\text{S}$  was 0.2 g  $\text{Na}_2\text{S}$ -S/L. This could be further investigated by analyzing the composition of the microbial community in the  $\text{Na}_2\text{S}$  batch reactors. Therefore, different microbial samples were taken at the end of batch experiments for microbial analysis through 16S rRNA sequencing. This could shed some light on whether there were specific microorganisms that promoted the increased  $\text{CH}_4$  yield or some other factors. It should be mentioned that the extracted DNAs were analyzed, and the sequencing results are received but the taxonomy alignments of dominant species should be done. The results of  $\text{Na}_2\text{SO}_4$  and  $\text{Na}_2\text{S}$  addition in AD process together with microbial analysis is going to be published in a high impact factor Journal. Furthermore, a similar experiment was conducted with different  $\text{Na}_2\text{S}$  concentration levels (mainly low concentrations) to see if the results can be replicated. These levels were 0.1 g  $\text{Na}_2\text{S}$ -S/L, 0.2 g  $\text{Na}_2\text{S}$ -S/L, and 0.4 g  $\text{Na}_2\text{S}$ -S/L which could confirm whether lower concentrations of  $\text{Na}_2\text{S}$  would increase the  $\text{CH}_4$  yield even further.

Table 3:  $\text{Na}_2\text{S}$  concentrations used for second batch experiments.

<b>level 1</b>	<b>level 2</b>	<b>level 3</b>	<b>Unit</b>
0.1	0.2	0.4	g S/L

Interestingly, the results were in consistent with first batch experiments with  $\text{Na}_2\text{S}$  addition. As it is shown in Figure 5, levels 2 and 3 i.e. 0.2 and 0.4 g  $\text{Na}_2\text{S}$ -S/L had increased the yield of  $\text{CH}_4$  by 8 and 8.5 % compared to the control, while level 1 (0.1 g  $\text{Na}_2\text{S}$ -S/L ) had similar yield as the control. Therefore, there is an optimum concentration for  $\text{Na}_2\text{S}$  addition to improve methane yield in AD process. According to the two series of batch experiments, the optimum sulfide concentration should be between 0.1 to 0.4 g S/L.

According to Figures 3 and 5, the  $\text{Na}_2\text{S}$  addition could cause a longer lag phase period for the methanogens. As mentioned previously, microbial analysis will reveal which microbial species are dominant in the batch experiments with lower  $\text{Na}_2\text{S}$  concentrations and which

microorganisms were stimulated which caused to higher methane production compared to higher levels of Na<sub>2</sub>S.

It should be noted that the above results are not published yet, and the manuscript is going to be prepared and submitted by the end of 2023 as the microbial samples are sequenced and ready to be analyzed.

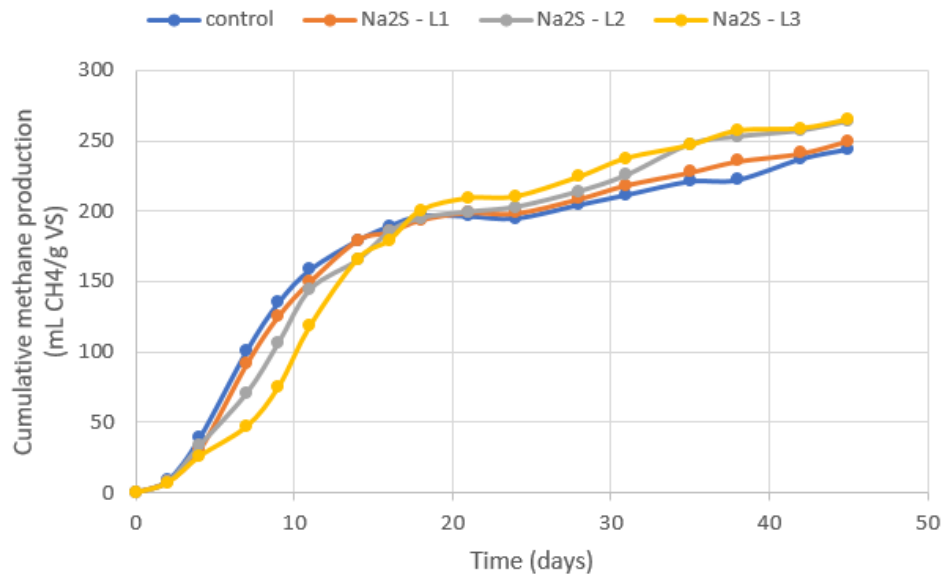


Figure 5 CH<sub>4</sub> production over time at three different levels of Na<sub>2</sub>S and control. The experiment was made with duplicates.

### 5.2.2 Lab-scale AD experiments in continuous mode:

According to the obtained results from batch-scale experiments, two continuous stirred tank reactors (CSTRs) were applied to be operated in parallel to investigate the effect of sulfur compounds in AD process in continuous mode. The aim was to precisely monitor the dynamic of the CSTRs in such disturbances i.e. sulfur compounds addition.

#### 5.2.2.1 CSTRs operation with sulfide salt (Na<sub>2</sub>S):

Two lab-scale continuous anaerobic digesters with working and total volumes of 1.8 and 2.0 L were run under mesophilic condition ( $37 \pm 1$  °C). The reactors were heated with silicone thermal jacket. The hydraulic retention time (HRT) were 18 days in both reactors. The feed to the reactors was supplied twice per day at the rate of 100 mL/day by a peristaltic pump. Organic loading rate of the feed was 2.22 g VS/L/d. During the whole period of CSTRs operation, gas composition, pH and VFAs concentration were measured two or three times a week. Furthermore, volume of the produced biogas was daily recorded via the liquid displacement method. The two CSTRs operated for 165 days (excluding the periods operational problems happened).

During the first 72 days (4 HRT), both CSTRs were fed with cattle manure (4% VS) to have identical reactors. As it is shown in Figure 6, there were a few operational problems in the first two weeks and finally after checking different factors, the tubes in the feeding pump were changed on day 17 and the CSTRs performance were improved. The difference between methane yield in R<sub>1</sub> and R<sub>2</sub> was higher than 10%. Therefore, on day 58, the inocula in the CSTRs were completely mixed and the CSTRs were re-inoculated again with the mixed inoculum. The performance of both CSTRs were similar (methane yield difference <10%) after cross inoculation.

According to the batch-scale experiments, the sodium sulfide addition in the range of 0.1 to 0.4 g Na<sub>2</sub>S-S/L were not inhibitory to methanogenesis. Therefore, the two CSTRs were operated within the same range obtained in batch-scale. On day 72, 0.1 and 0.2 g Na<sub>2</sub>S-S/L were added directly to R<sub>1</sub> and R<sub>2</sub>, respectively in a single injection. The two CSTRs were fed consciously with 0.1 and 0.2 g Na<sub>2</sub>S-S/L to keep the sulfide levels in the reactors constant. As it can be seen in Figure 6, the methane yield decreased in both R<sub>1</sub> and R<sub>2</sub> immediately after sulfide addition and gradually increased to similar methane yields before sulfide addition on day 80. Interestingly, the methane yield increased up to 153.73 mL-CH<sub>4</sub> g<sup>-1</sup> VS L<sup>-1</sup> on day 88. The methane yield increased by adding 0.2 g Na<sub>2</sub>S-S/L in R<sub>2</sub> during period II compared to period I without any sulfide salt addition while there was no effect in R<sub>1</sub> in presence of 0.1 g Na<sub>2</sub>S-S/L. The obtained results in continuous operation were consistent with batch-scale experiments confirming the positive effect of sulfide in anaerobic digestion process in specific amount of 0.2 g S/L. The experiments were continued with higher concentrations of sulfide salt. On day 114, the concentration of sulfide in R<sub>1</sub> and R<sub>2</sub> were increased to 0.2 and 0.4 g Na<sub>2</sub>S-S/L, respectively. As it is shown in Figure 6, in R<sub>1</sub> the methane yield decreased to 86.71 mL-CH<sub>4</sub> g<sup>-1</sup> VS L<sup>-1</sup> for 2 days after new sulfide level and recovered to the same yield before sulfide addition. While in R<sub>2</sub>, the methane yield declined to 49.44 mL-CH<sub>4</sub> g<sup>-1</sup> VS L<sup>-1</sup> on day 116 and increased gradually to 99.22 mL-CH<sub>4</sub> g<sup>-1</sup> VS L<sup>-1</sup> after 6 days (day 20). It can be concluded that in period III, adaptation period in R<sub>2</sub> (sulfide change from 0.2 to 0.4 g S/L) was higher than R<sub>1</sub> (sulfide change from 0.1 to 0.2 g S/L). The methane yield in R<sub>1</sub> increased up to 160.75 mL-CH<sub>4</sub> g<sup>-1</sup> VS L<sup>-1</sup> which was 4.6% higher than maximum methane yield achieved in period II for R<sub>2</sub> with the same sulfide concentration (0.2 g S/L). In general, the methane yield in R<sub>1</sub> (0.2 g Na<sub>2</sub>S-S/L) was higher than R<sub>2</sub> containing 0.4 g Na<sub>2</sub>S-S/L. Therefore, it can be concluded that optimum concentration of sulfide for improved methane production was 0.2 g Na<sub>2</sub>S-S/L. It is assumed that this optimum concentration can enhance the activity of methanogens and probably suppress growth of SRBs. On the other hand, sulfur can be served by methanogens

for growth. Therefore, further microbial analysis is necessary to approve the enrichment of specific methanogens and SRBs. It should be noted that to avoid any sulfide loss in the feed bottle (sulfide is slightly soluble in water), the reactors were fed manually once per day with cattle manure containing different sulfide levels added in different periods of experiment. To confirm the effect of manual feeding for sulfide salts addition, the reactors were automatically fed by the pumps through feed bottles containing sulfide salts from day 130 to 134. As it is shown in Figure 6, the methane yield dropped immediately which proved the effect of sulfide volatility. Manual feeding of the reactors was continued again on day 135. The CSTRs reached to steady state condition and the average methane yield in R<sub>1</sub> was 135.19 mL-CH<sub>4</sub> g<sup>-1</sup> VS L<sup>-1</sup> which was 25.8% higher than that of R<sub>1</sub> at the end of period III.

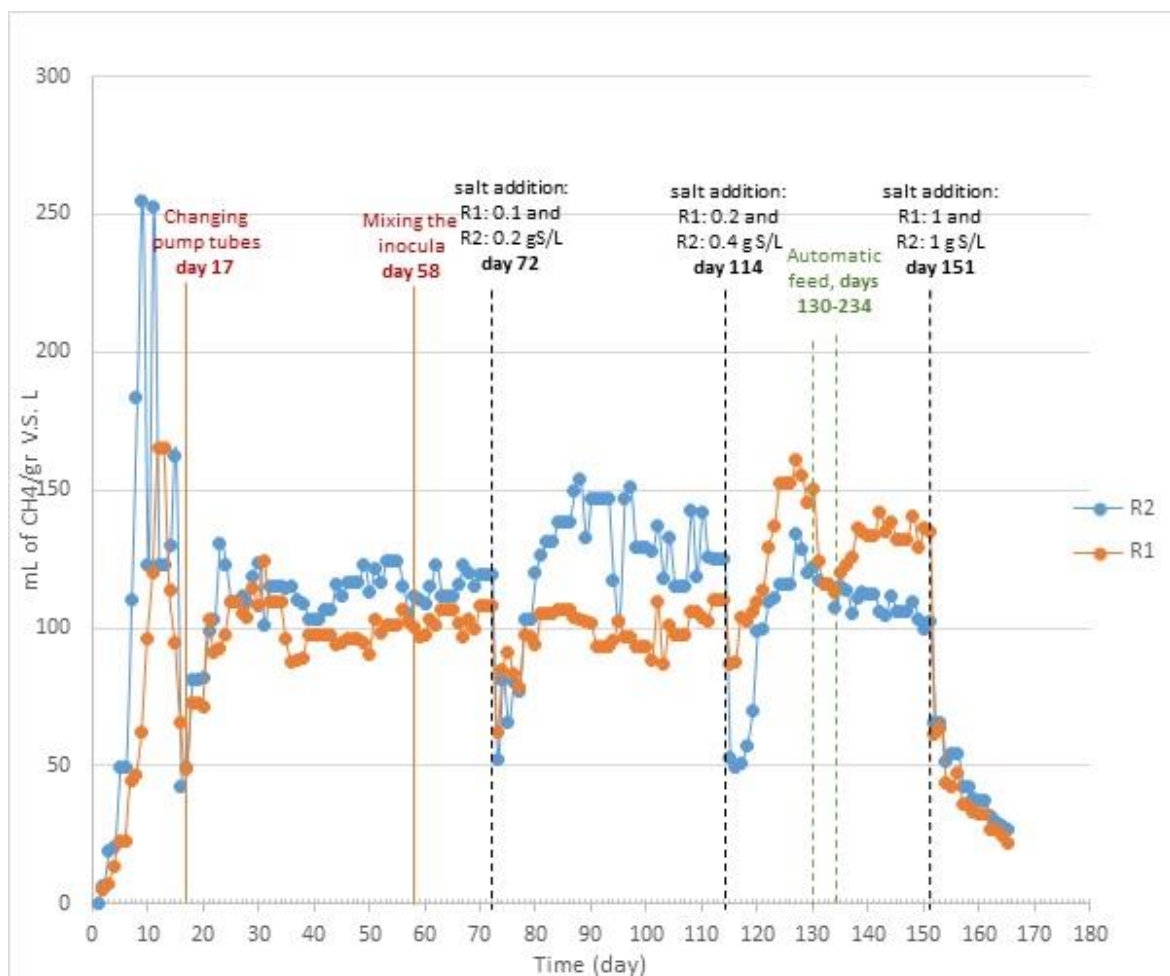


Figure 6 methane yield during operation of two CSTRs (R<sub>1</sub> and R<sub>2</sub>) with different sulfide salts concentrations

Finally, the two CSTRs were exposed to 1 g Na<sub>2</sub>S-S/L on day 151 as the highest level of sulfide concentration. As it is shown in Figure 6, both R<sub>1</sub> and R<sub>2</sub> were inhibited because of high sulfide concentration which caused inhibition of the methanogens and methane yields declined immediately after Na<sub>2</sub>S addition in period IV. These batch and continuous experiments showed

that addition of low concentration of sulfide salt (0.2 g S/L) can enhance methane production during AD process. It should be noted that microbial samples were taken at the end of each experimental periods for both R<sub>1</sub> and R<sub>2</sub> to analyze the microbial community and investigate the most dominant species in each operational condition. The experimental results which were shown in this report to study the effect of sulfur compounds on AD process are not published yet and they are going to be published in 2-3 high impact factor journals in Elsevier. Therefore, the presented data should be kept confidential.

## **6. Test and validation of the SPECTRO sensor**

The experimental set up applied to test Spectro Biogas sensor consisted of a continuously stirred tank reactor (CSTR) with 9.0 L total and 7.5 L working volumes. The bottom plate of the reactor was changed and modified in order to install the SPECTRO sensor in the reactor and provide direct interfacing of the mass spectrometer with the biomass for real-time analysis. Furthermore, the top plate of the reactor was also modified to have proper sampling ports, gas recirculation etc. The Spectro Biogas sensor was fully set up on 17<sup>th</sup> of October 2022. Therefore, some initial tests were designed to test the sensor performance in detection of different gases involved in AD process. Different gases such as N<sub>2</sub>, H<sub>2</sub>, CO<sub>2</sub> and CH<sub>4</sub> were injected in the headspace (gas phase) of the reactor to evaluate if the sensor output signals were affected/changed by the gas injections. It should be noted that during testing the sensor with different gases there were some problems in data acquisition/collection by sensor software and many data were lost because of these disconnections. Sometimes the sensor was also disconnected locally in Spectro Company, and the data was lost. The initial tests with different gases were conducted in abiotic condition i.e. the reactor was filled with distilled water. In order to provide efficient contact between injected gases and liquid phase, the reactor configuration was modified. A circulation loop was considered on the top plate of the reactor in order to recirculate the injected gases and accelerate reaching to steady state condition. Before injecting any of the gases, the N<sub>2</sub> was purged in the reactor in order to have anaerobic condition as real condition in biogas production process. As the sensor could detect N<sub>2</sub> in the liquid phase, therefore the N<sub>2</sub> signal was increases immediately after N<sub>2</sub> purging process (at ~1240 minutes) as it is shown in Figure 7. The output response of the other gases is shown in Figure 8.

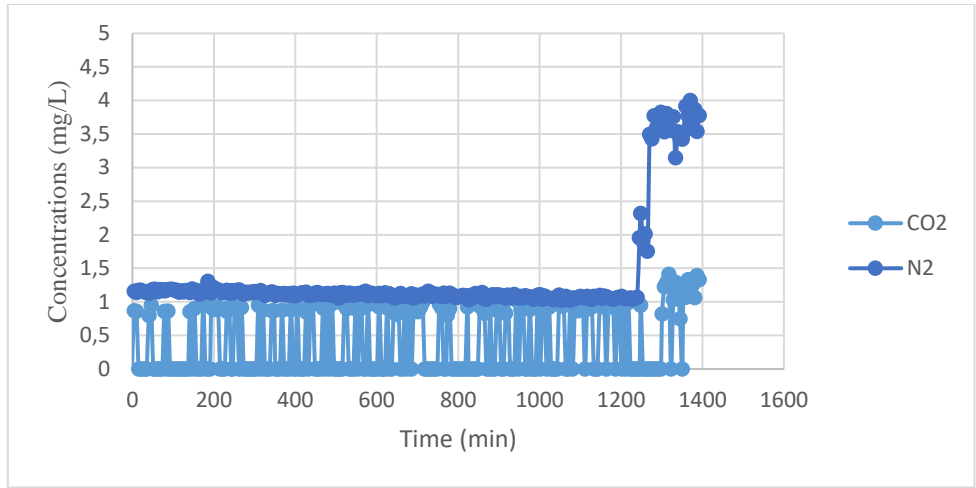


Figure 7 concentration of N<sub>2</sub> and CO<sub>2</sub> in the liquid phase of the CSTR

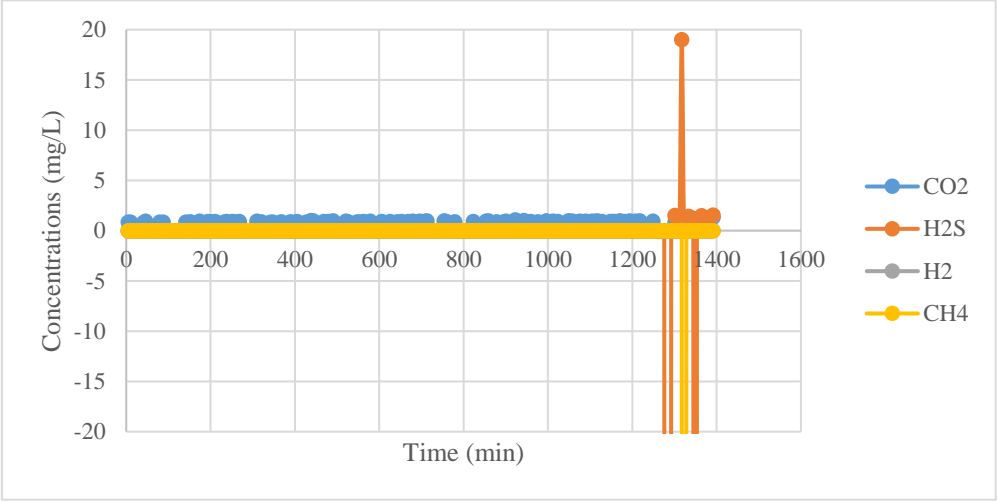


Figure 8 concentration of CO<sub>2</sub>, H<sub>2</sub>S, H<sub>2</sub> and CH<sub>4</sub> in the liquid phase of the CSTR

As it can be seen in Figure 8, there were some errors in H<sub>2</sub>S and CH<sub>4</sub> measurements while N<sub>2</sub> was purged. As the most dominant gases involved in AD process are CH<sub>4</sub>, CO<sub>2</sub> and H<sub>2</sub>, respectively therefore they were considered on the other hand it was not possible to test the sensor with H<sub>2</sub>S and NH<sub>3</sub> as we were prohibited because safety reasons to carry pure H<sub>2</sub>S and NH<sub>3</sub> in the lab to inject them to the reactor headspace. Therefore, it was decided to check the sensor performance in terms of H<sub>2</sub>S and NH<sub>3</sub> measurements during biotic operation of the reactor for biogas production by addition of Na<sub>2</sub>S and NH<sub>4</sub>Cl to the digester as a disturbance. The trend of NH<sub>3</sub> concentration in the liquid phase detected by sensor is shown in Figure 9.

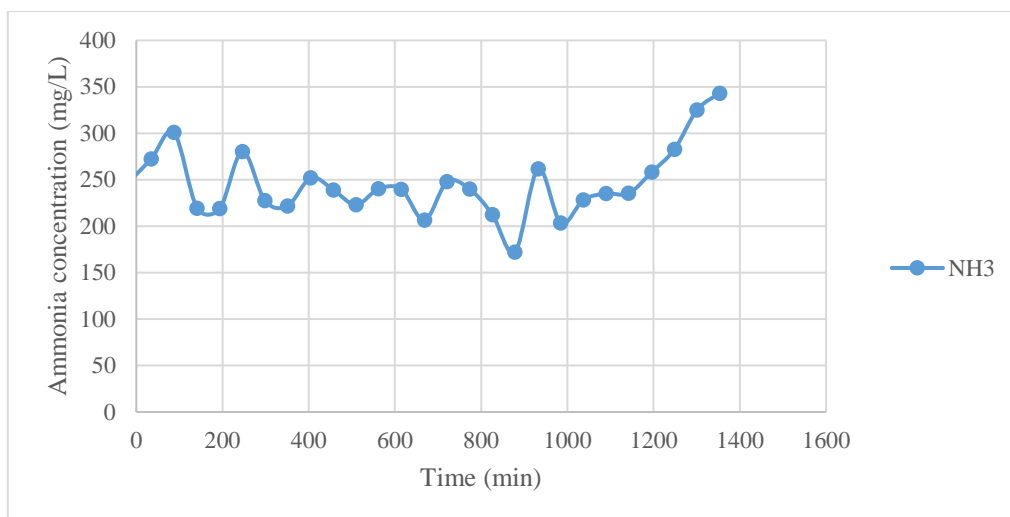


Figure 9 concentration of CO<sub>2</sub>, H<sub>2</sub>S, H<sub>2</sub> and CH<sub>4</sub> in the liquid phase of the CSTR

In Figure 10, the concentration of different gases in the liquid phase is shown while no gas was injected in the reactor headspace.

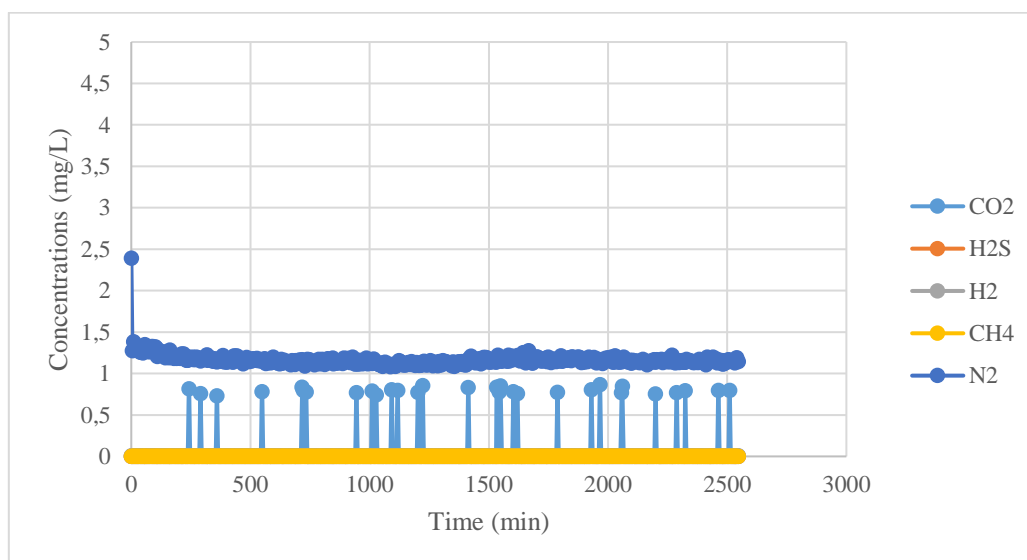


Figure 10 concentration of different gases in the liquid phase of the CSTR without any gas injection in reactor headspace

### 6.1 Sensor validation in detecting H<sub>2</sub> concentration in the liquid phase:

After purging the N<sub>2</sub> in the reactor, the N<sub>2</sub> flow was stopped at 374 minutes and H<sub>2</sub> was injected into the headspace of the reactor (5% V/V) as it is shown in figures 11 and 12. The concentration of H<sub>2</sub> after equilibrium was increased from 0.006 to 0.012 mg/L by injecting 5% V/V H<sub>2</sub> in the reactor.

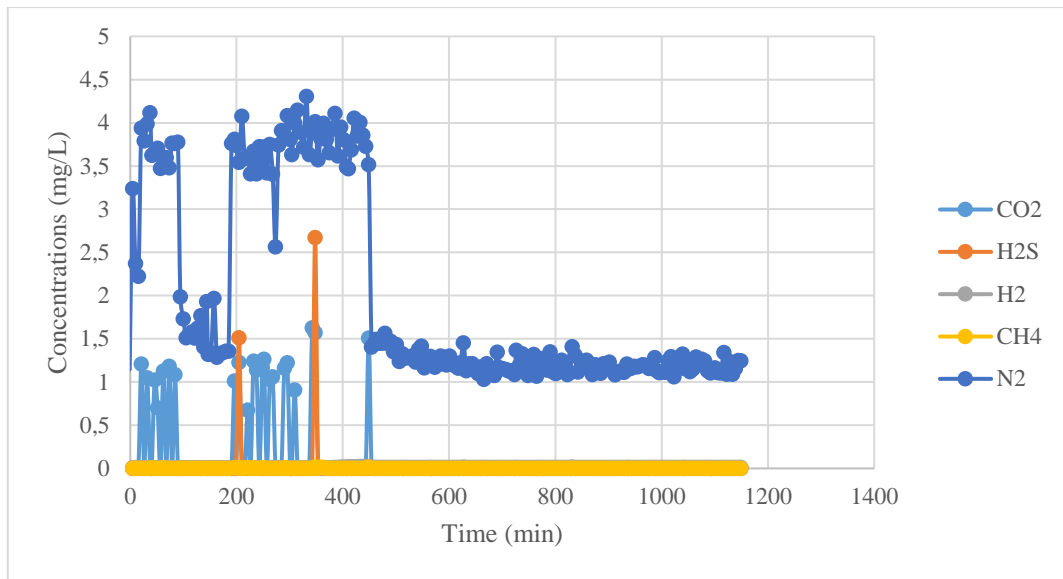


Figure 11 concentration of different gases in the liquid phase of the CSTR with 5% V/V H<sub>2</sub> injection in the reactor headspace

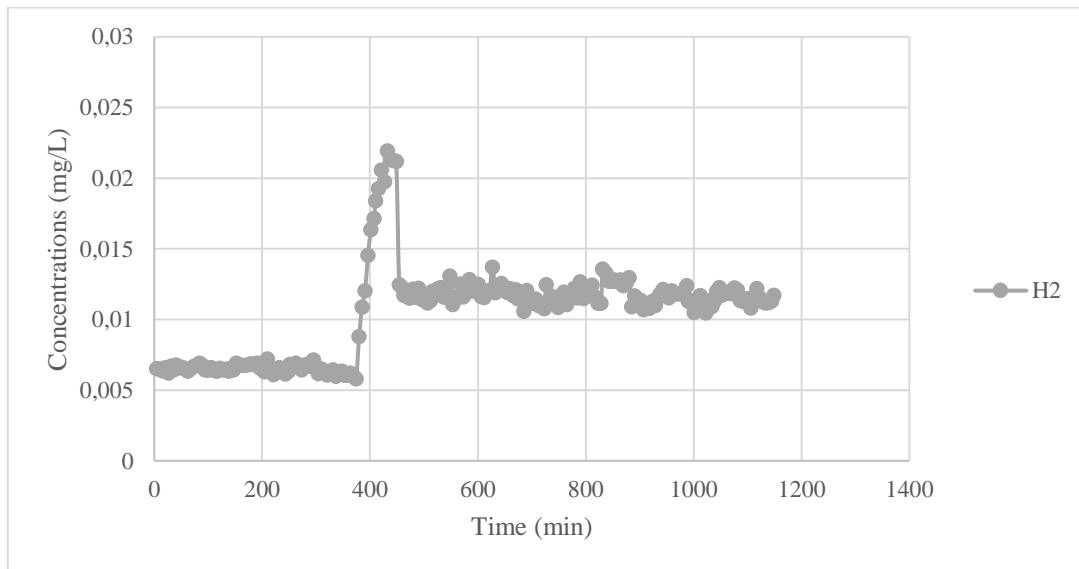


Figure 12 concentration of H<sub>2</sub> in the liquid phase of the CSTR with 5% V/V H<sub>2</sub> injection in the reactor headspace

Higher concentrations of H<sub>2</sub> (10%, 15%, 20%, 25 and 30% V/V) were added to the reactor headspace step by step and the GC measurements were shown in Table 4. However, unfortunately again there was a problem in data collection by SPECTRO sensor and even the sensor was running, no data was recorded and collected because of miscommunication between sensor and its software. Therefore, the sensor data of these set of experiments were lost. The problem with sensor was solved the day after and the data were collected again after sensor troubleshooting. As it was mentioned the H<sub>2</sub> composition was increased up to 30% V/V in the reactor headspace. By comparing Figures 12 and 13, the H<sub>2</sub> concentration in the first 39 minutes (after sensor connection) was around 0.1 mg/L (Figure 13) while after 5% V/V H<sub>2</sub> injection

was around 0.012 mg/L which confirms the sensor output is increased by increase of H<sub>2</sub> concentration in the reactor head space. Unfortunately, the data between 5 and 30% V/V H<sub>2</sub> injections was not recorded and collected by the sensor.

Table 4. GC measurements from reactor headspace for different H<sub>2</sub> injections

Injected gas (H <sub>2</sub> ) in the reactor headspace (% V/V)	Gas (H <sub>2</sub> ) composition based on GC
5	5.6507
10	12.32095
15	18.7315
20	24.82255
25	31.78415
30	40.40985

As it is shown in Figures 13 and 14, another problem was occurred during H<sub>2</sub> injection. The reactor stirrer stopped after some hours working and caused the H<sub>2</sub> concentration to decrease from 0.1 to 0.04 mg/L. The stirrer was operated again after 1000 minutes, and the output signal returned to the previous level (0.1 mg/L). As it can be seen in Figures 13 and 14, this problem happened again and the H<sub>2</sub> signal dropped immediately after stirrer stopped as the gas bubbles retention time will decrease without stirring.

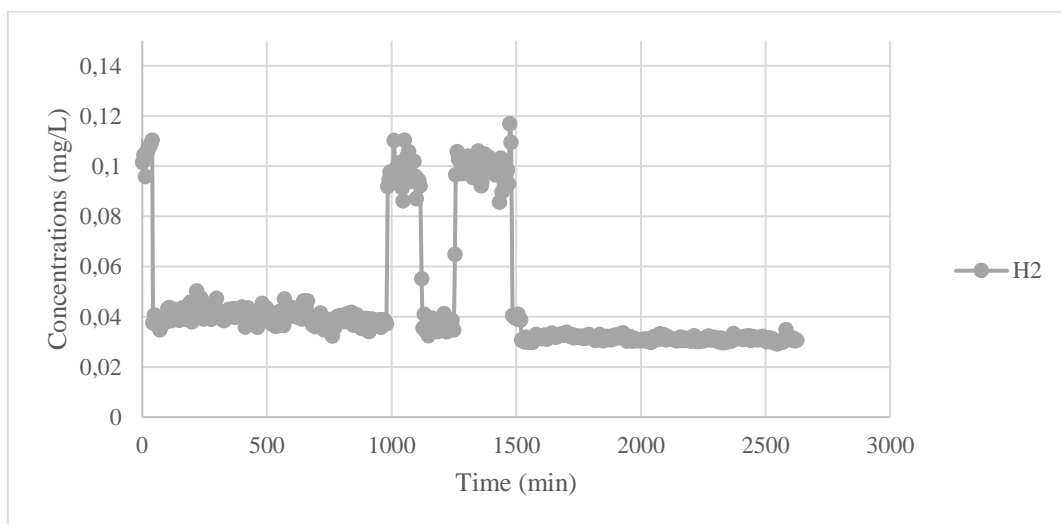


Figure 13 concentration of H<sub>2</sub> in the liquid phase of the CSTR after 30% V/V H<sub>2</sub> injection in the reactor headspace

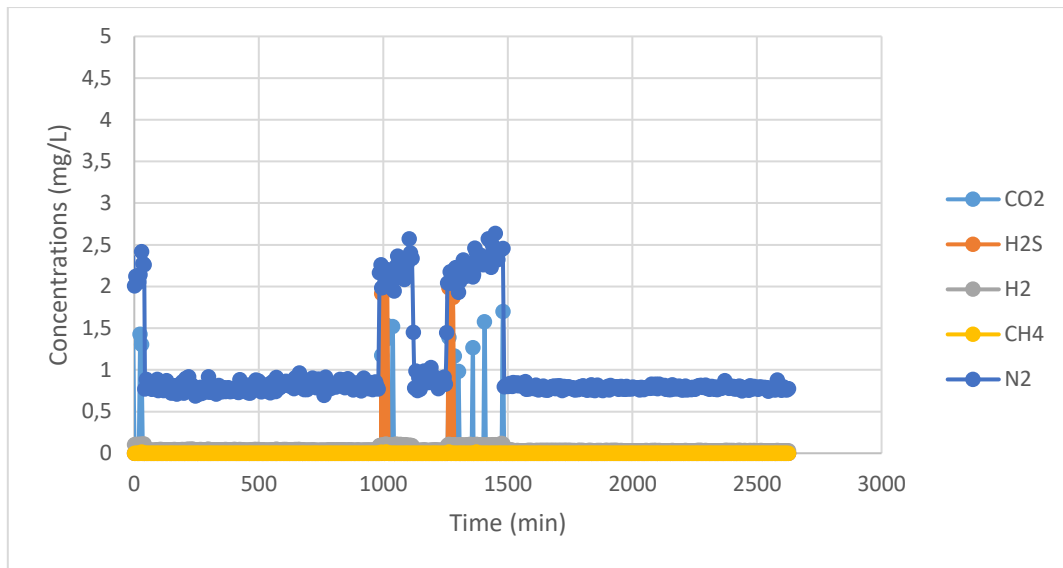


Figure 14 concentration of different gases in the liquid phase of the CSTR after 30% V/V H<sub>2</sub> injection in the reactor headspace

The same experiments were repeated with 5 to 30% V/V H<sub>2</sub> injection in the reactor headspace but as it can be seen in Figure 15, the data was not recorded by sensor again due to local disconnection of sensor in Spectro Company and the data was lost.

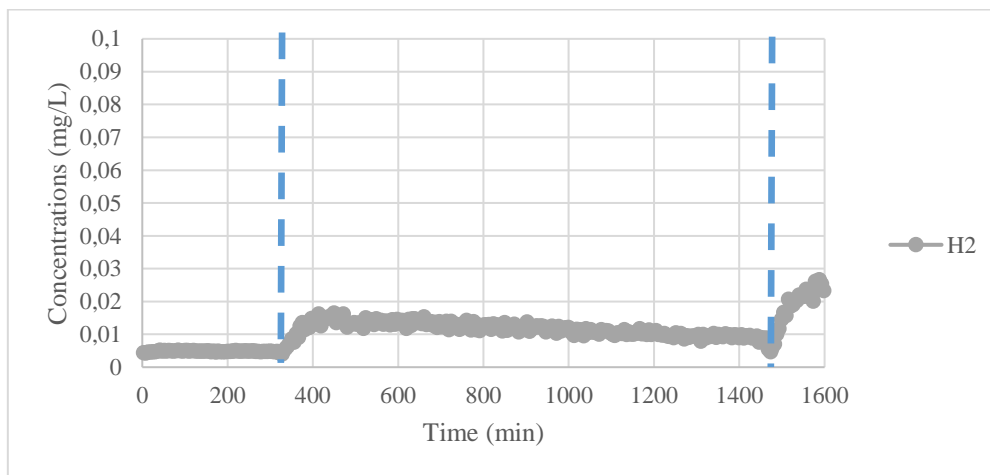


Figure 15 concentration of H<sub>2</sub> in the liquid phase of the CSTR after 5-15% V/V H<sub>2</sub> injection in the reactor headspace

## 6.2 Sensor validation in detecting CO<sub>2</sub> concentration in the liquid phase:

After the initial tests with H<sub>2</sub> injections, the sensor performance was evaluated with CO<sub>2</sub> injections in the reactor headspace. As it is shown in the Figure 16, the CO<sub>2</sub> concentration was increased in the headspace of the reactor from 5% to 30% V/V every 2 hours. However, it was concluded that the injections time intervals should be longer in order to reach the equilibrium between liquid and gas phase. The GC measurements were performed in order to compare the

GC results with sensor results. The output signals for the other gases during CO<sub>2</sub> injections are shown in Figure 17.

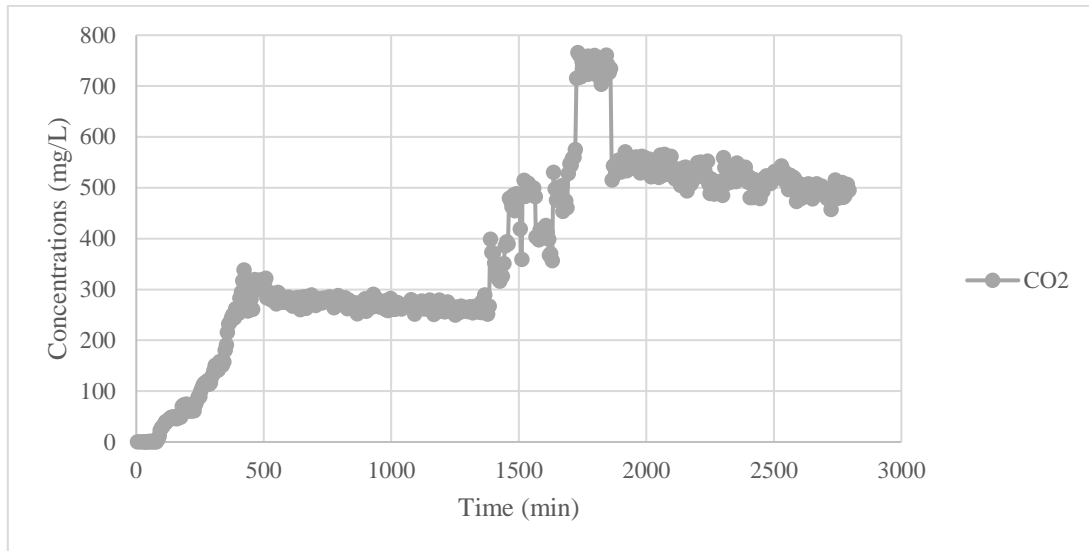


Figure 16 concentration of CO<sub>2</sub> in the liquid phase of the CSTR by injecting 5 to 30 % V/V CO<sub>2</sub> injection in the reactor headspace.

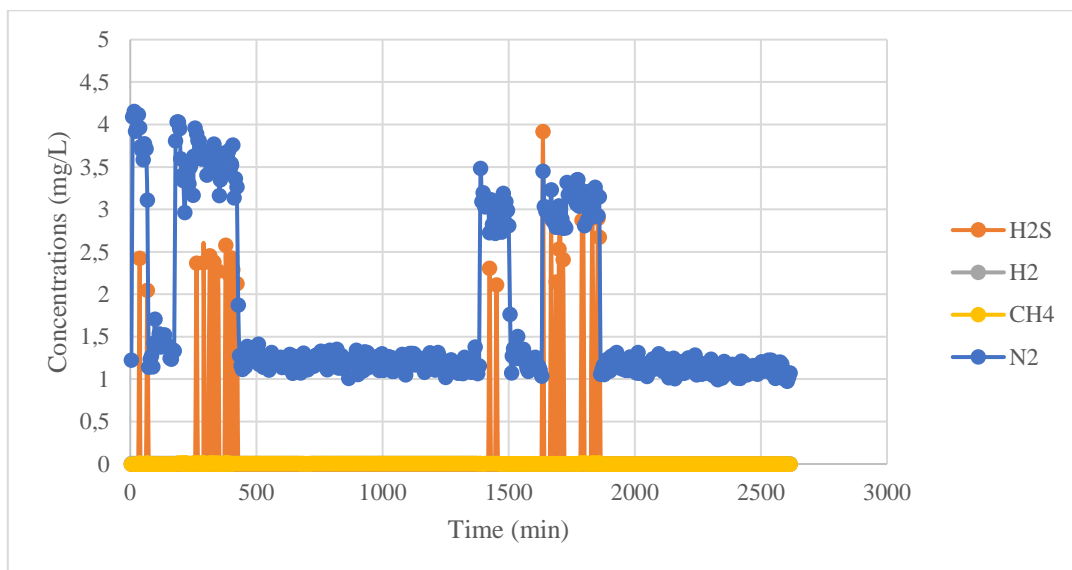


Figure 17 concentration of different gases in the liquid phase of the CSTR by injecting 5 to 30 % V/V CO<sub>2</sub> injection in the reactor headspace.

The results shown in Figure 16 were divided in two separate graphs, i.e. Figures 18 (obtained results up to 600 min) and 19 (collected results between 1300 to 2500 min). As it is shown in Figure 18, the CO<sub>2</sub> concentration in the liquid phase was increased after injecting higher CO<sub>2</sub> (5 to 20% V/V) in the headspace. After injecting 20% V/V CO<sub>2</sub> to the headspace (at 400 min) and the reactor was operated in the same condition over the night until the next day. The reactor stirrer stopped again during this period, and it restarted again at 1388 minutes (Figure 19).

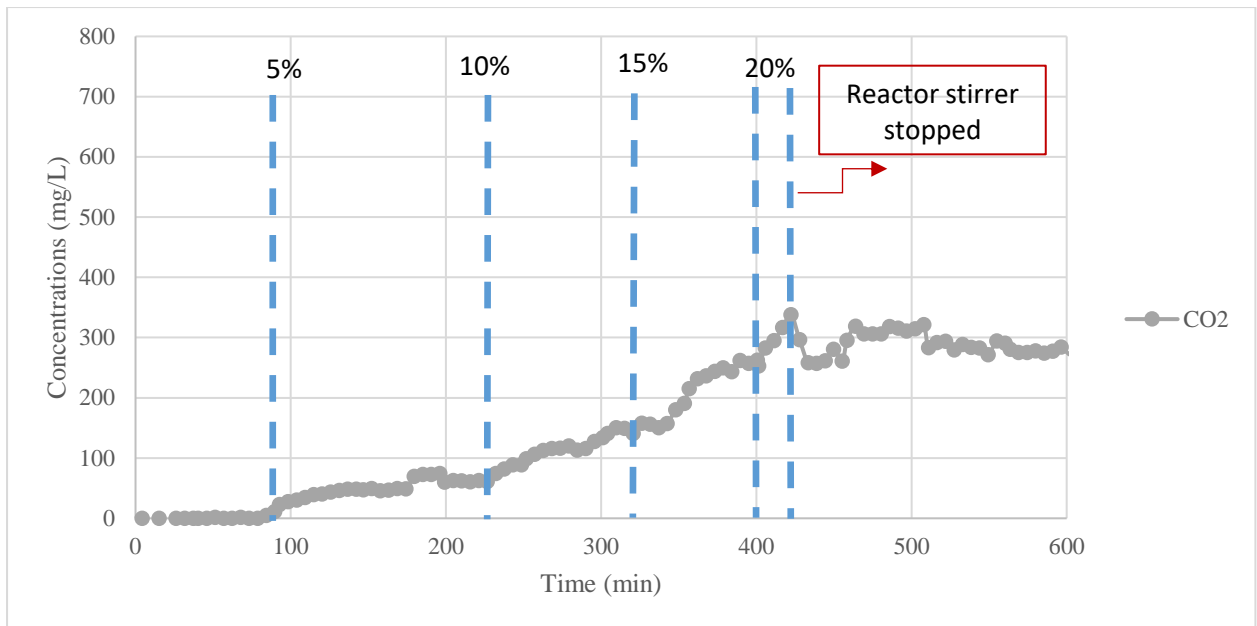


Figure 18 concentration of CO<sub>2</sub> in the liquid phase of the CSTR by injecting 5 to 20 % V/V CO<sub>2</sub> injection in the reactor headspace.

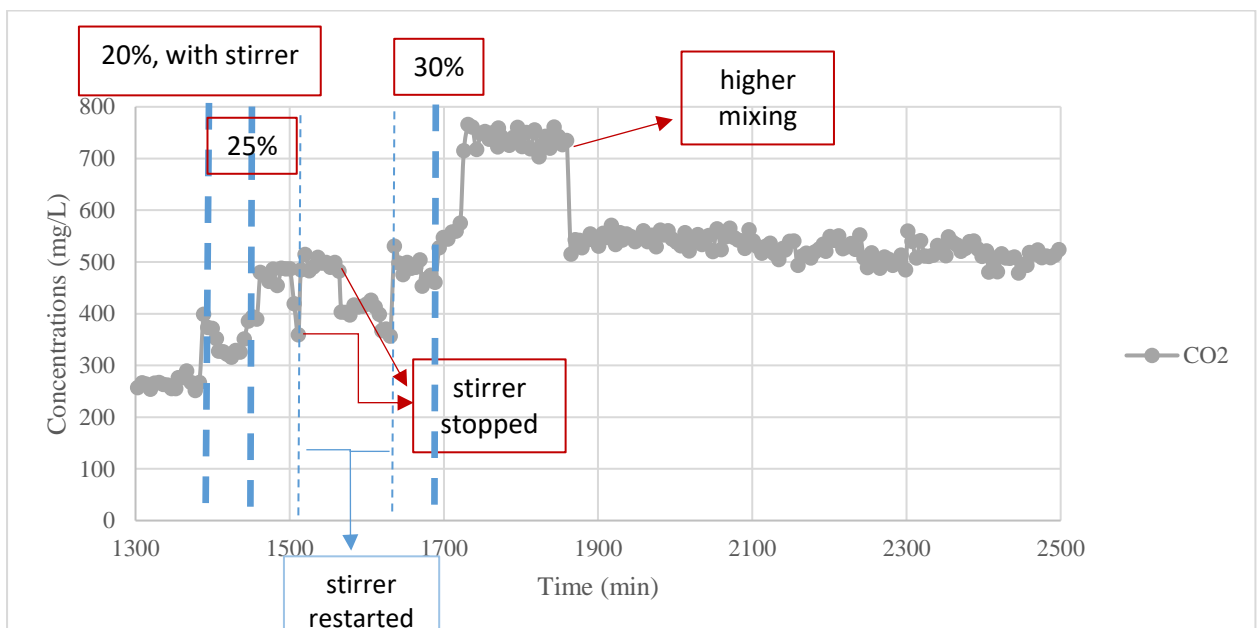


Figure 19 concentration of CO<sub>2</sub> in the liquid phase of the CSTR by injecting 20 to 30 % V/V CO<sub>2</sub> injection in the reactor headspace.

As it is shown in Figure 19, the stirrer stopped several times during different injections. In order to solve the problem with the stirrer, a new Arduino board (as a microcontroller) was ordered to separate stirring system from other devices such as gas meter, pH meter etc. and control the reactor stirrer without any problem. The stirrer operated continuously afterwards. The concentration of CO<sub>2</sub> in the liquid phase was calculated based on GC results and compared with sensor results in Table 5.

Table 5. The CO<sub>2</sub> concentration in liquid phase calculated based on GC measurements.

Concentration of CO <sub>2</sub> in the liquid based on GC (mg/L)	Recorded data by sensor (mg/L)	Sensor to GC Ratio LGA/GC
31.96	67.76920646	2.120236
188.09	306.3346792	1.628696
379.06	738.1157792	1.947248

In another test, the sensor was tested with 5, 15, 20, 25 and 30% V/V and the recorded data by sensor are presented in Figure 20. The GC measurements for each CO<sub>2</sub> concentration were shown in Table 6. Unfortunately, again the communication between sensor and its software was lost and the data from 20 to 30% V/V CO<sub>2</sub> injection were lost. Therefore, there are only two data points, which can be compared to GC results (Table 7).

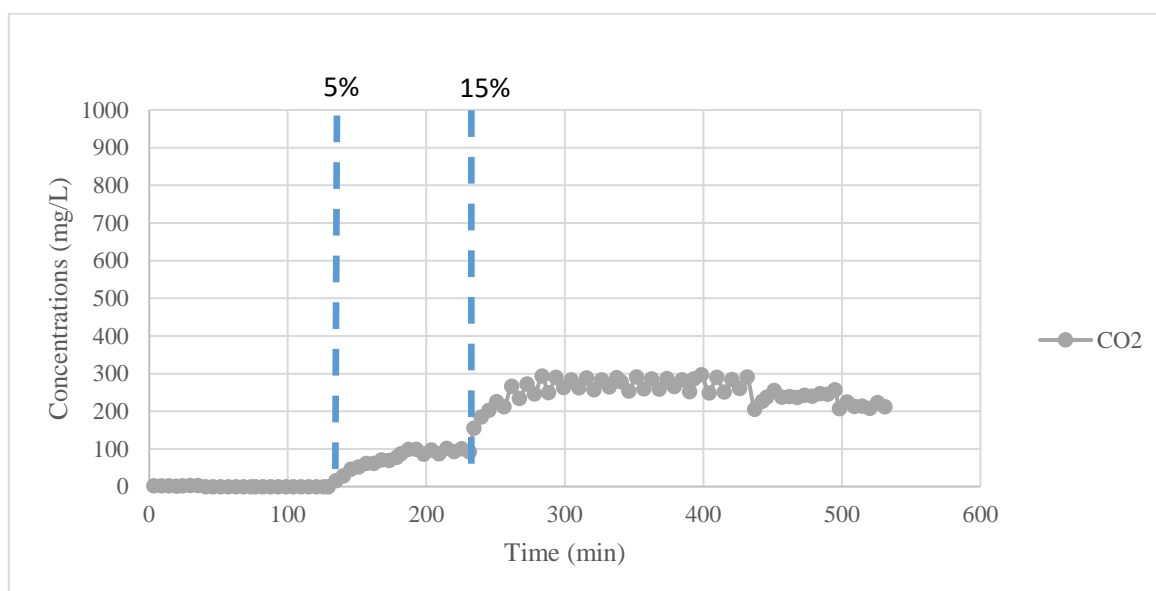


Figure 20 concentration of CO<sub>2</sub> in the liquid phase of the CSTR by injecting 5 to 15 % V/V CO<sub>2</sub> injection in the reactor headspace.

Table 6. GC measurements from reactor headspace for different CO<sub>2</sub> injections

Injected gas (CO <sub>2</sub> ) in the reactor headspace (% V/V)	Gas (CO <sub>2</sub> ) composition based on GC
5	2.45125
15	9.8106
20	10.3711
25	12.93575
30	14.4145

Table 7. The CO<sub>2</sub> concentration in liquid phase calculated based on GC measurements.

Concentration of CO <sub>2</sub> in the liquid based on GC (mg/L)	Recorded data by sensor (mg/L)	Sensor to GC Ratio LGA/GC
37.61	94.32388229	2.507921
80.71	274.2643134	3.398197

In another experiment, the sensor was tested with 5, 10, 20 and 30% V/V and the recorded data by sensor are presented in Figure 21, but unfortunately due to miscommunication between sensor and its software, the data of 5 and 30 % V/V CO<sub>2</sub> injection were lost. After troubleshooting by Spectro Company, the sensor was tested again with 20 and 30% V/V and the results are shown in Figure 22. The comparison between GC and sensor results are presented in Table 8.

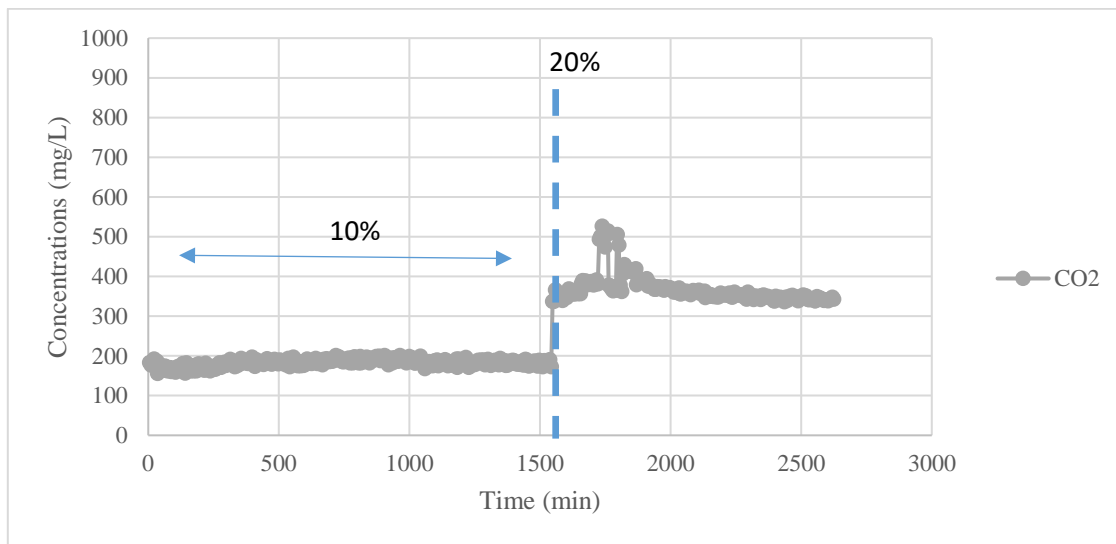


Figure 21 concentration of CO<sub>2</sub> in the liquid phase of the CSTR by injecting 10 to 20 % V/V CO<sub>2</sub> injection in the reactor headspace.

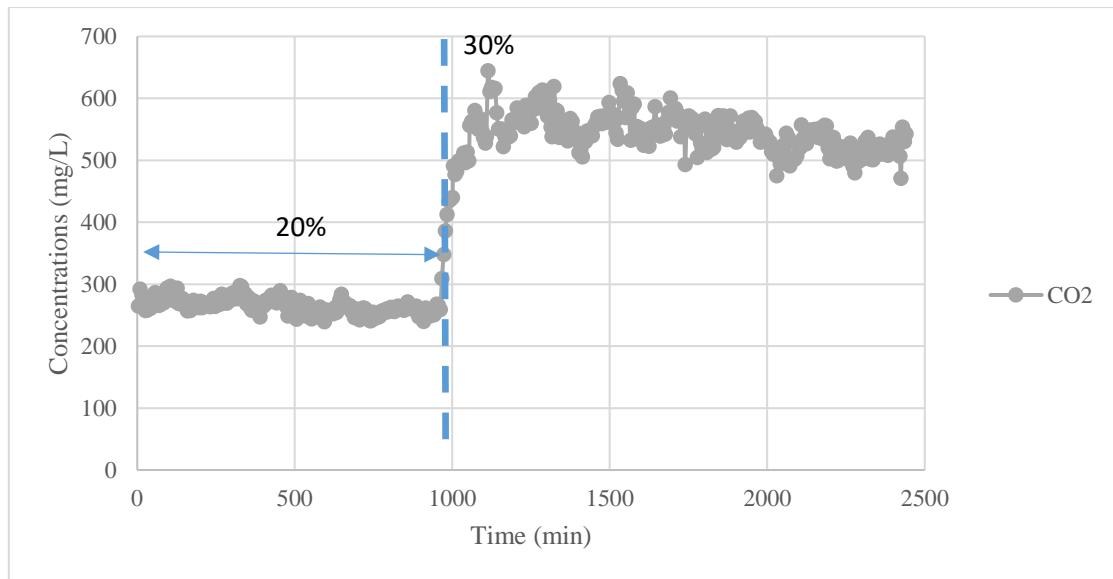


Figure 22 concentration of CO<sub>2</sub> in the liquid phase of the CSTR by injecting 20 to 30 % V/V CO<sub>2</sub> injection in the reactor headspace.

Table 8. The CO<sub>2</sub> concentration in liquid phase calculated based on GC measurements.

Concentration of CO <sub>2</sub> in the liquid based on GC (mg/L)	Recorded data by sensor (mg/L)	Sensor to GC Ratio LGA/GC
140.74	255.9723	1.81878
251.96	525.2262	2.084539

Finally, after the sensor was restarted again by Spectro Company, another CO<sub>2</sub> test was conducted to compare sensor results with GC measurements. The only difference in this test is that the reactor was purged by N<sub>2</sub> for 20-30 minutes before each injection with higher CO<sub>2</sub> concentration. Therefore, the CO<sub>2</sub> concentration dropped to 0 because of N<sub>2</sub> purging (Figure 23). As it can be seen, the sensor output signal is increasing as the concentration of CO<sub>2</sub> in the headspace is increasing. The comparison between calculated results based on GC measurements and recorded data by sensor are shown in Table 9 and Figure 24. According to these results, the CO<sub>2</sub> concentration detected by sensor is 2.32 times (in average) higher than obtained results based on GC results. It means that sensor is overestimated compared to GC results.

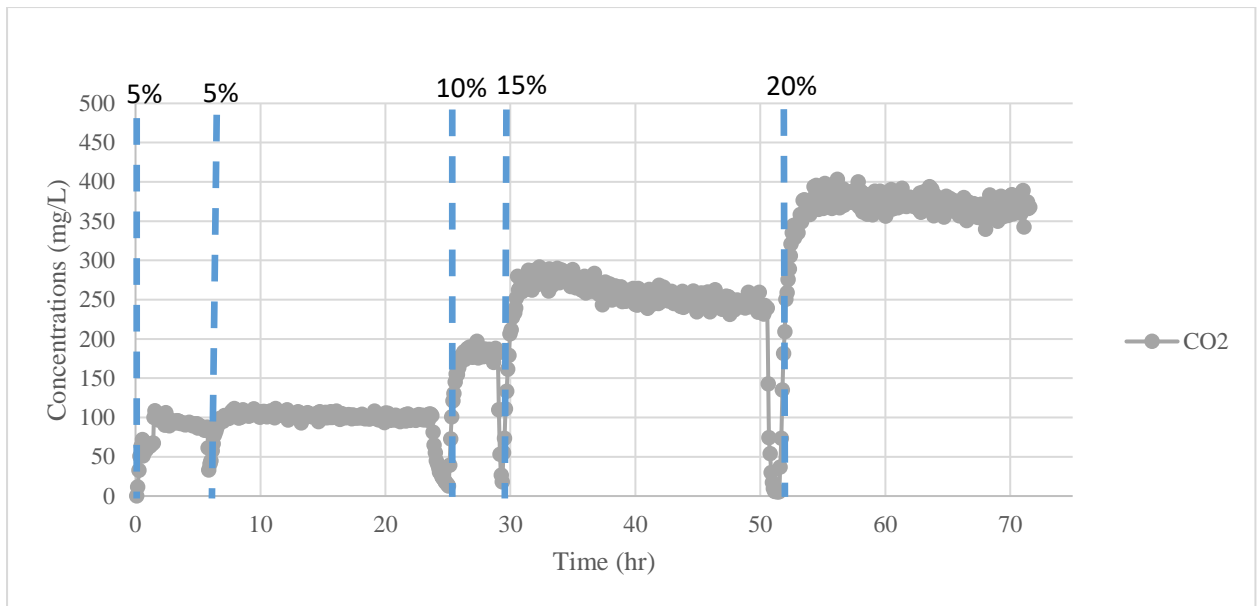


Figure 23 concentration of CO<sub>2</sub> in the liquid phase of the CSTR by injecting 5 to 20 % V/V CO<sub>2</sub> injection in the reactor headspace.

Table 9. The CO<sub>2</sub> concentration in liquid phase calculated based on GC measurements.

Concentration of CO <sub>2</sub> in the liquid based on GC (mg/L)	Recorded data by sensor (mg/L)	Sensor to GC Ratio LGA/GC
35.12	89.06618	2.54
50.54	102.3466	2.02511
79.87	182.079	2.279726
99.51203	278.6616	2.80028
177.1569	345.1093	1.948043

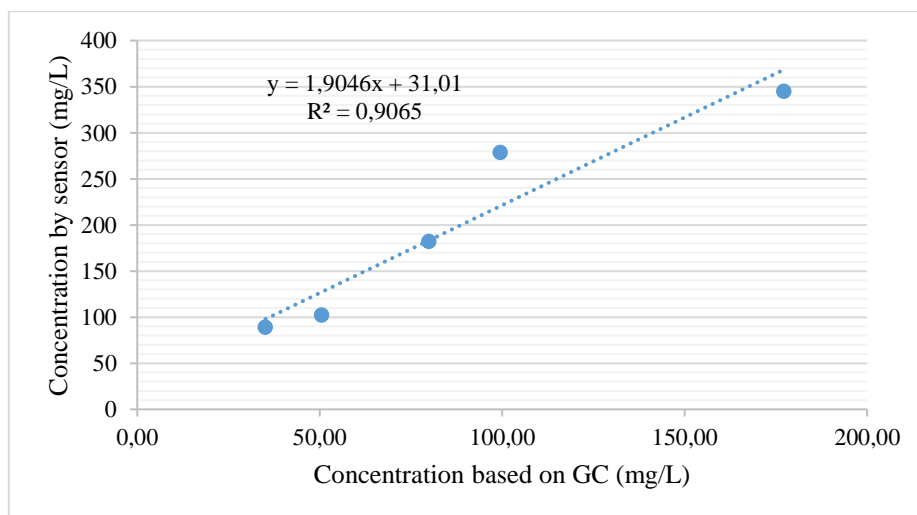


Figure 24 Comparison between sensor and expected CO<sub>2</sub> concentration based on GC.

### 6.3 Sensor validation in detecting CH<sub>4</sub> concentration in the liquid phase:

After testing the sensor with CO<sub>2</sub>, the sensor was also tested with CH<sub>4</sub>. For these experiments, the water in the reactor was replaced with fresh distilled water to ensure there is no CO<sub>2</sub> dissolved in the liquid phase. The reactor headspace was purged with N<sub>2</sub> before starting the CH<sub>4</sub> injections. CH<sub>4</sub> was added in different concentrations of 10, 20 and 30% and the results are shown in Figure 25. At the same GC measurements were conducted to evaluate sensor performance in CH<sub>4</sub> detection. The obtained results based on GC analysis and SPECTRO sensor are reported in Table 10.

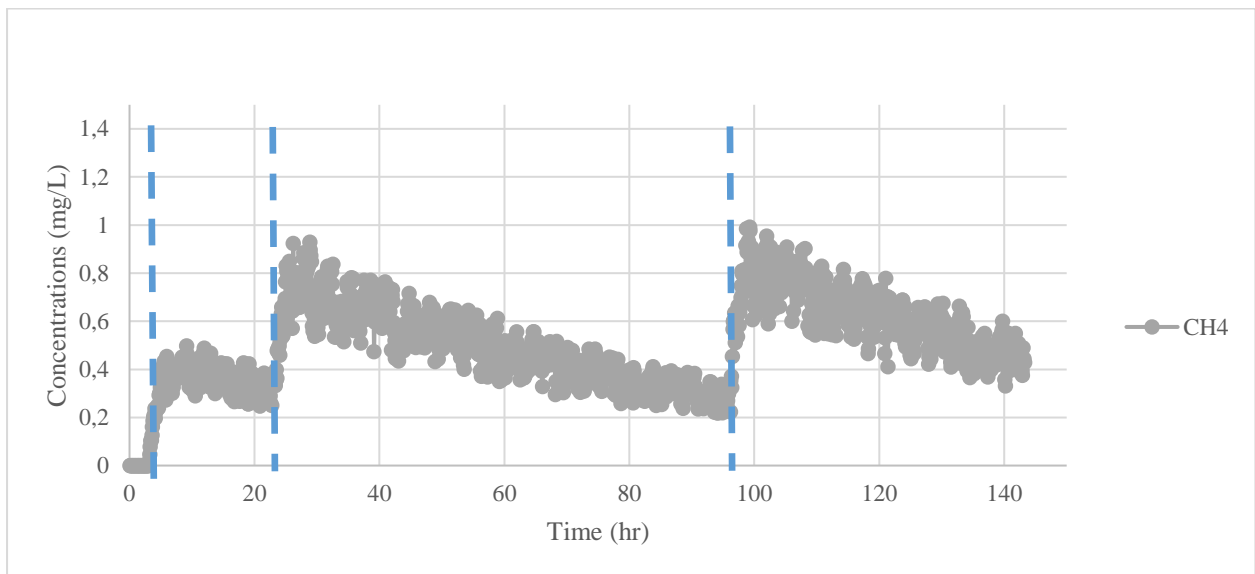


Figure 25 concentration of CH<sub>4</sub> in the liquid phase of the CSTR by injecting 10 to 30 % V/V CH<sub>4</sub> injection in the reactor headspace.

Table 10. The CH<sub>4</sub> concentration in liquid phase calculated based on GC measurements.

Concentration of CH <sub>4</sub> in the liquid based on GC (mg/L)	Recorded data by sensor (mg/L)	Sensor to GC Ratio LGA/GC
3.73	0.315741	0.084537
6.30	0.565809	0.089811

According to the results presented in Table 10, the sensor CH<sub>4</sub> measurements were underestimated compared to the expected CH<sub>4</sub> concentration based on GC, i.e. the GC to sensor ratio was 11.48 in average.

Similar experiments were conducted to evaluate the sensor in CH<sub>4</sub> detection. The only difference in this test is that the reactor was purged with N<sub>2</sub> for 20 minutes before each CH<sub>4</sub> injection. The results are presented in Figure 26 and 27 (focusing only on the first 50 hr). Different concentrations of 5, 10, 15, 20 and 25 % V/V were injected to the reactor headspace, respectively. The comparison between calculated results based on GC measurements and

recorded data by sensor are shown in Table 11 and Figure 28. Like previous test with different CH<sub>4</sub> concentrations, the sensor results were underestimated compared to GC results. the GC to sensor ratio was 8.19 in average which was lower than previous experiments (GC/LGA=11.48).

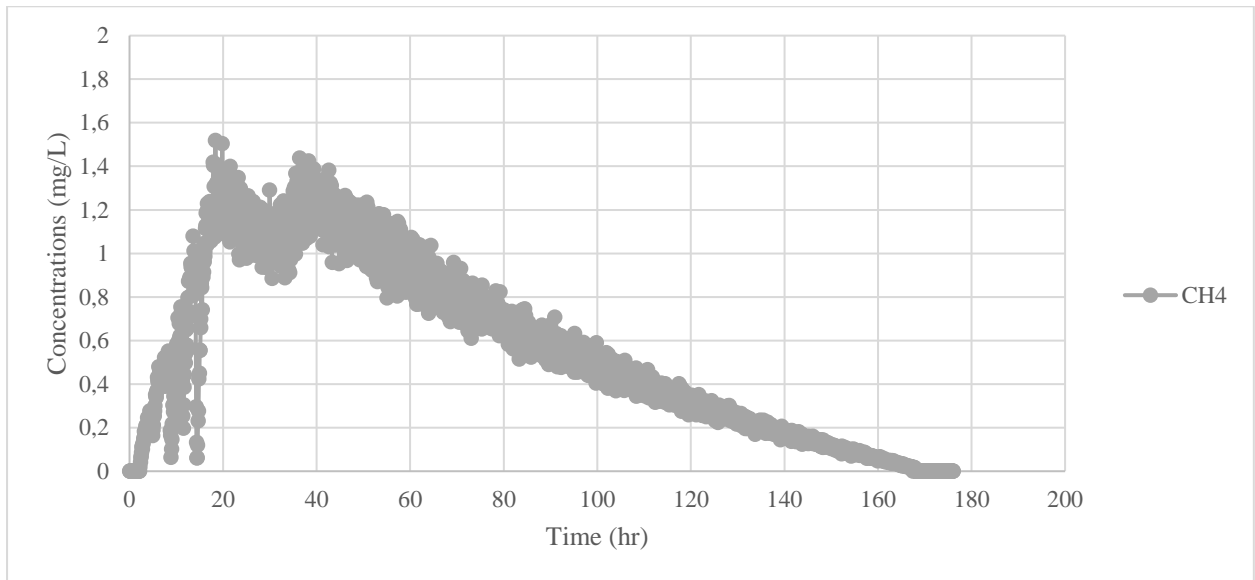


Figure 26 concentration of CH<sub>4</sub> in the liquid phase of the CSTR by injecting 5 to 20 % V/V CH<sub>4</sub> injection in the reactor headspace.

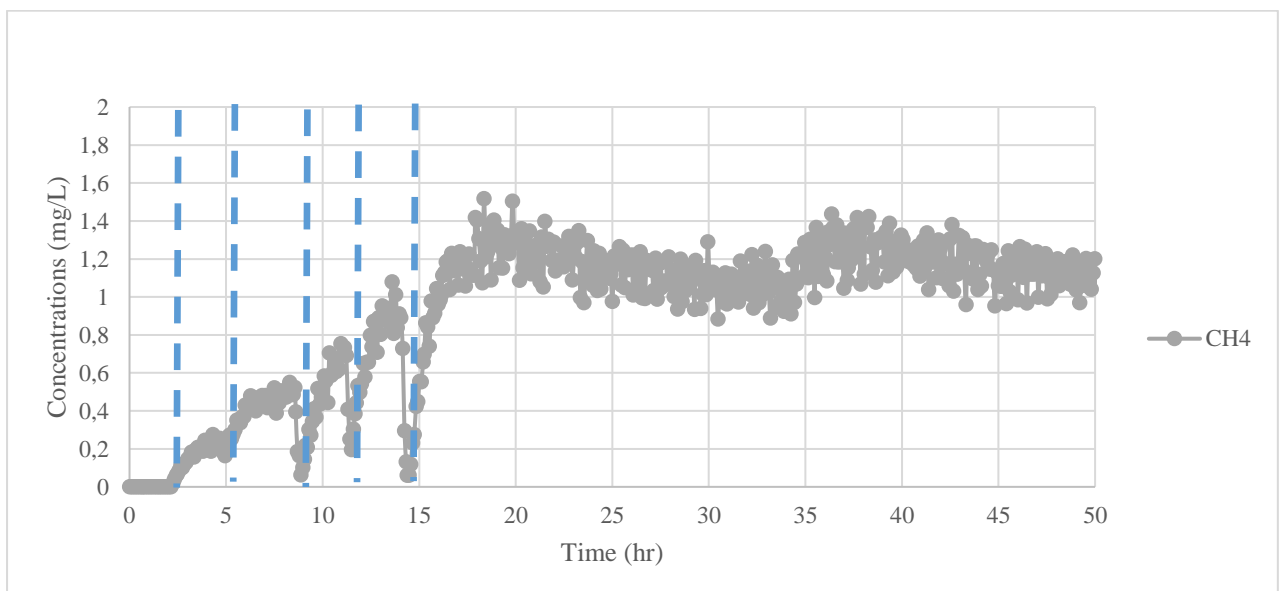


Figure 27 concentration of CH<sub>4</sub> in the liquid phase of the CSTR by injecting 5 to 20 % V/V CH<sub>4</sub> injection in the reactor headspace (focusing on the first 50 hr)

Table 11. The CH<sub>4</sub> concentration in liquid phase calculated based on GC measurements.

Concentration of CH <sub>4</sub> in the liquid based on GC (mg/L)	Recorded data by sensor (mg/L)	Sensor to GC Ratio LGA/GC
1.60	0.2246	0.140013
3.59	0.4818	0.13417
5.60	0.6343	0.113256
6.81	0.9254	0.135874
11.12	1.0930	0.09825

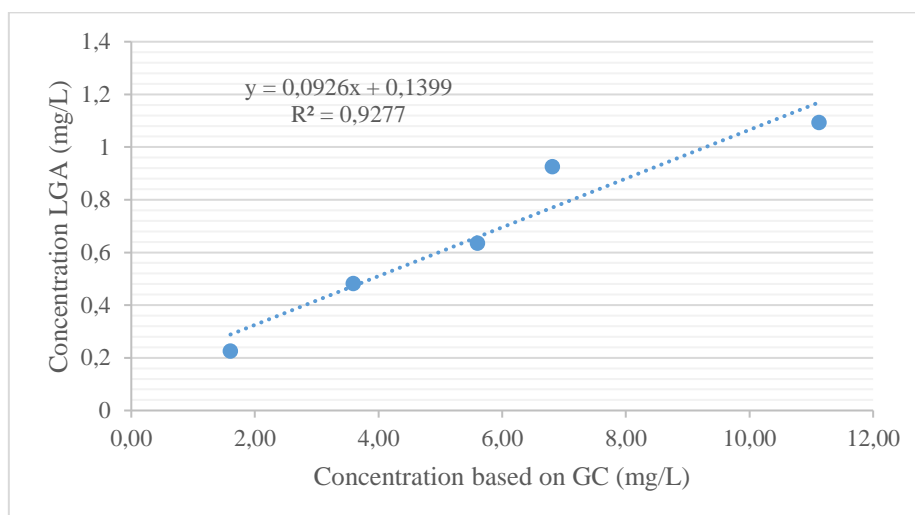


Figure 28 Comparison between sensor and expected CH<sub>4</sub> concentration based on GC.

#### 6.4 Repeating the sensor validation in detecting H<sub>2</sub> concentration in the liquid phase:

At the end, the sensor was evaluated again with H<sub>2</sub> gas as the previous efforts were incomplete because of sensor disconnection. The sensor was tested by injection of 5, 10, 15, 20, 25 and 30% V/V H<sub>2</sub> in the reactor headspace, respectively. In these experiments, the reactor was purged with N<sub>2</sub> for 20 minutes before each H<sub>2</sub> injection as it is shown in Figure 29.

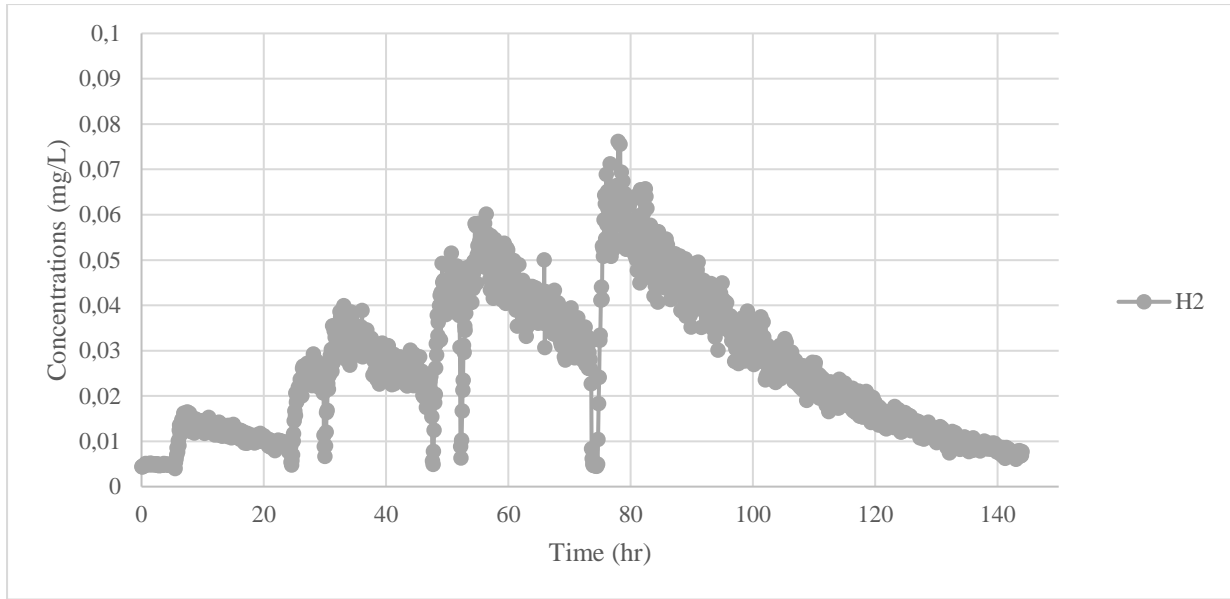


Figure 29 concentration of H<sub>2</sub> in the liquid phase of the CSTR by injecting 5 to 20 % V/V H<sub>2</sub> injection in the reactor headspace.

The comparison between calculated results based on GC measurements and recorded data by sensor are shown in Table 12 and Figure 30.

Table 12. The H<sub>2</sub> concentration in liquid phase calculated based on GC measurements.

Concentration of H <sub>2</sub> in the liquid based on GC (mg/L)	Recorded data by sensor (mg/L)	Sensor to GC Ratio LGA/GC
0.11	0.0140	0.125949
0.23	0.0244	0.106567
0.39	0.0334	0.086713
0.53	0.0444	0.08442
0.82	0.0488	0.05971
1.02	0.0591	0.057826

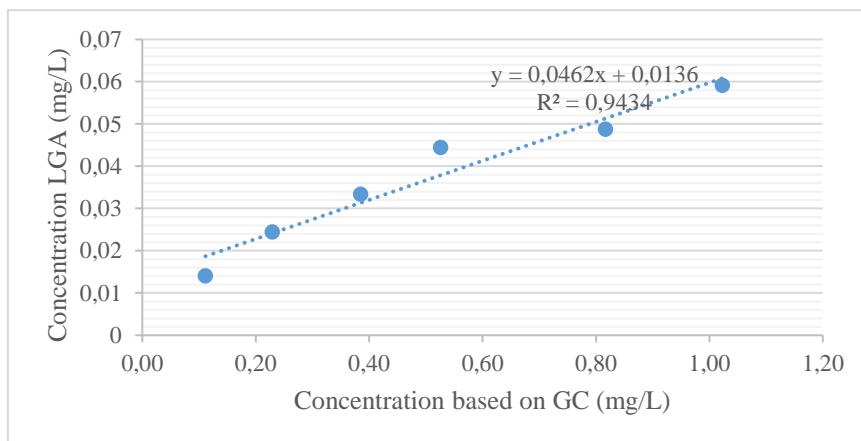


Figure 30 Comparison between sensor and expected H<sub>2</sub> concentration based on GC.

According to these results, the H<sub>2</sub> concentration detected by sensor are underestimated compared to the expected results calculated based on GC measurements. It means that the GC to sensor ratio was 12.46 in average. According to Figure 30, it seems that two different calibration curves for low and high range H<sub>2</sub> concentration should be used to re-calibrate the SPECTRO sensor.

According to the results obtained in this section, it can be concluded that the sensor is underestimated for H<sub>2</sub> and CH<sub>4</sub> measurements and overestimated for CO<sub>2</sub> measurements which can be improve by re-calibration of the sensor. As it was mentioned previously, because of the safety reasons, it was impossible to test the sensor with H<sub>2</sub>S and NH<sub>3</sub> injections to the reactor headspace as they are considered as highly toxic gases. The performance of sensor in H<sub>2</sub>S and NH<sub>3</sub> was monitored in real reactor operation for biogas production and the results are shown in section 5.

### **6.5 Evaluation of sensor performance by different gas mixtures**

Before starting the reactor operation with anaerobic digestion process, a synthetic gas mixture (used for biogas upgrading process) composed of 23% CH<sub>4</sub>, 15% CO<sub>2</sub> and 62% H<sub>2</sub> to resemble a mixture of biogas (~60% CH<sub>4</sub> and 40% CO<sub>2</sub>) and H<sub>2</sub> was injected in different volumes (14%, 24% and 33 % V/V) in the reactor headspace to evaluate the sensor performance in simultaneous presence of different gases. In the previous experiments, only pure gases of CH<sub>4</sub>, CO<sub>2</sub> and H<sub>2</sub> were tested. The recorded data by sensor were shown in Figures 31 and 32. The results showed that the concentration of CO<sub>2</sub>, H<sub>2</sub> and CH<sub>4</sub> were increased by increasing the volume of the gas mixture injected to the reactor headspace. Therefore, the sensor was ready to be tested with real biogas production process.

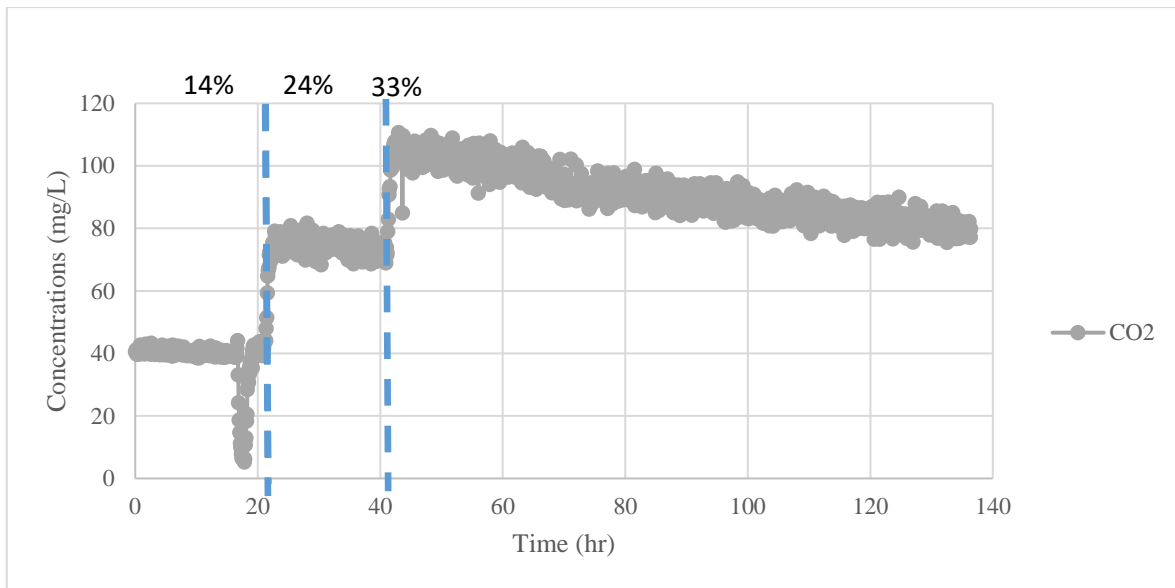


Figure 31 concentration of CO<sub>2</sub> in the liquid phase of the CSTR by injecting 14, 24 and 33 % V/V synthetic gas mixture in the reactor headspace.

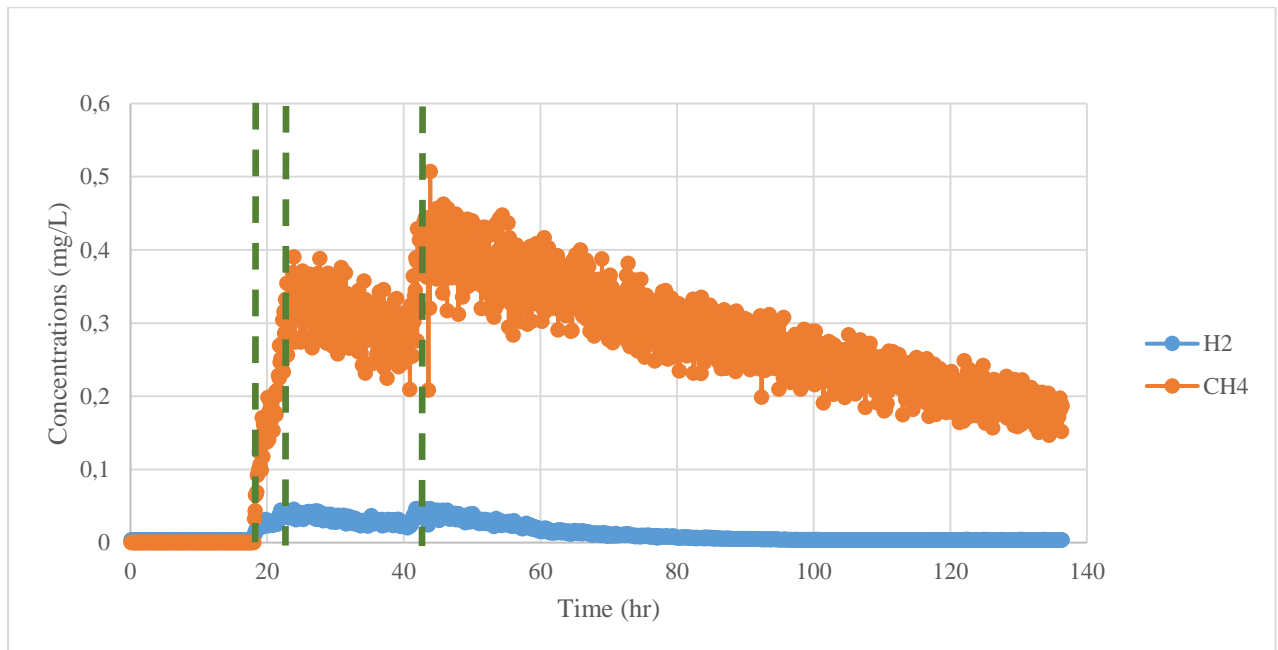


Figure 32 concentration of H<sub>2</sub> and CH<sub>4</sub> in the liquid phase of the CSTR by injecting 14, 24 and 33 % V/V synthetic gas mixture in the reactor headspace.

It should be noted that the sensor was tested many times with pure gases (CO<sub>2</sub>, H<sub>2</sub> and CH<sub>4</sub>) and sometime the data was lost because of some errors in the sensor software. Therefore, only the interesting and promising results were included in the Spectro Biogas final report.

## 7. Use of the SPECTRO sensor for gas-liquid mass transfer parameter determination

In-situ gas fermentation and upgrading are regarded as promising but to optimize approaches to increase the performance and product quality of anaerobic digestion reactors. In these scenarios, reliable online measurement systems to determine the concentration of dissolved gases are necessary to further validate models used for process optimization. Thus, the scope of the experiment presented in this section was to validate the accuracy of measurements of the SPECTRO sensor while injecting a gas directly into the liquid phase of the reactor through a sparging device. The SPECTRO sensor could be very practical in gas-liquid systems such as biogas upgrading or syngas methanation as it can measure the dissolved gases in the liquid phase. Therefore, a sparger was designed and installed to increase the surface contact between gas and liquid phase compared with section 3 that different gases were injected directly to the headspace of the reactor and the gases were recirculated in the reactor through a pump.

### 7.1 Methods

A circular horn-shaped, tubular (OD 8 mm, ID 6 mm), stainless steel sparger (see Figure 33) with four 0.6 mm holes was placed at the bottom of the reactor. The holes were located on the upper part of the sparger tubes, at the end and in the middle of the total length of the tubes making the “horns”. The sparger tubes were positioned 3 cm above the bottom of reactor while the diameter of the sparger was about 2/3 of the internal reactor diameter so that the stirrer blades rotate just above the sparger to maximize bubble breakage and avoid holes clogging.



Figure 33 View from above of the installed gas sparger in the used reactor. In the center of the bottom of the reactor is visible the SPECTRO sensor

The experimental set-up was disassembled to install the gas sparger and the set-up is shown in Figure 34.



Figure 34 Experimental set-up during sparger installation

The experiment consisted in injecting a gaseous mix (40% H<sub>2</sub>, 30% CO, 20% CO<sub>2</sub>, 10% N<sub>2</sub>) with a flow rate of 280 ml min<sup>-1</sup> in the reactor filled up to 7.5 L with distilled water for 40-50 minutes. The experiment was carried out at two stirring speeds, namely 60 rpm (Experiment A) and 30 rpm (Experiment B). The reactor temperature was set to 37 °C. To validate the measure of the concentration of dissolved gases (H<sub>2</sub> and CO<sub>2</sub>) provided by the SPECTRO sensor, an independent and already validated methodology (named in this report GC-method) was used (Grimalt-Aleman et al., 2020). Liquid samples (20 ml per sample) were collected every 2 minutes and injected into 25 ml bottles sealed with gas-tight pierceable serum caps. The bottles were then placed in an oven at 105 °C for more than 3 hours, after which the gas phase composition of the bottles was analyzed with a gas chromatograph (Thermo Fisher Scientific, US) equipped with a thermal conductivity detector (described in section 2.2.1) and calibrated with gas mixtures with known composition. The number of moles of the gas species was then calculated by means of the ideal gas law and divided by the volume of the corresponding liquid samples to retrieve the gas concentration in the liquid samples at the sampling time.

## 7.2. Results and discussion

Experiment A was carried out two times (See Figures 35 and 36) as during the first attempt (Experiment A.1) the SPECTRO sensor failed just before starting the experiment as well as to provide a reliable statistical basis (a total of three experiments were carried out) to prove the robustness of the GC-method as a reference to evaluate the measure accuracy of the SPECTRO sensor.

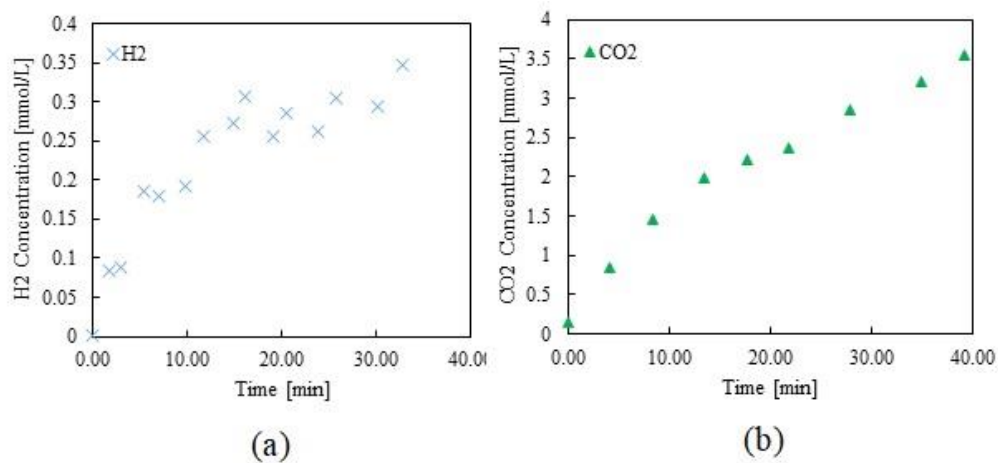
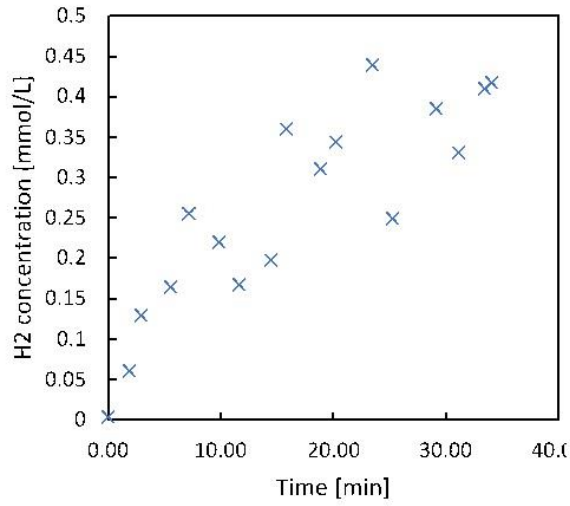
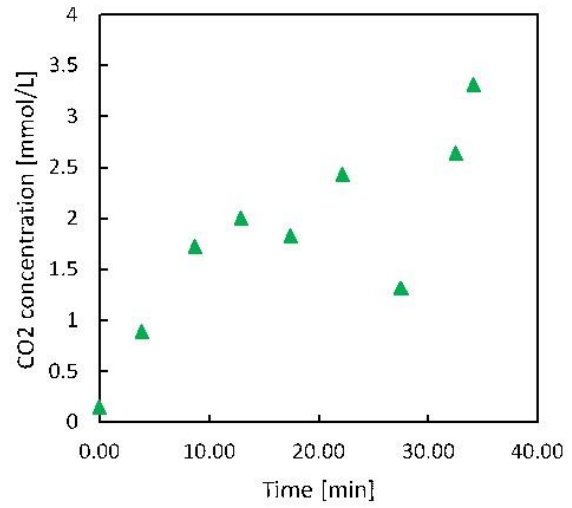


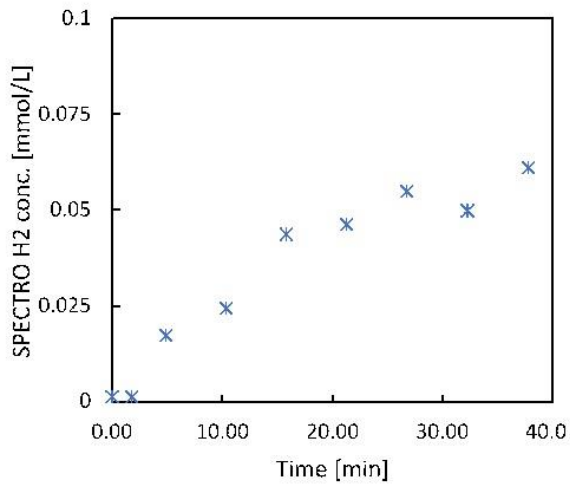
Figure 35 (a) H<sub>2</sub> and (b) CO<sub>2</sub> concentration determined by GC-method during gas sparging time in Experiment A.1 (stirring speed 60 rpm).



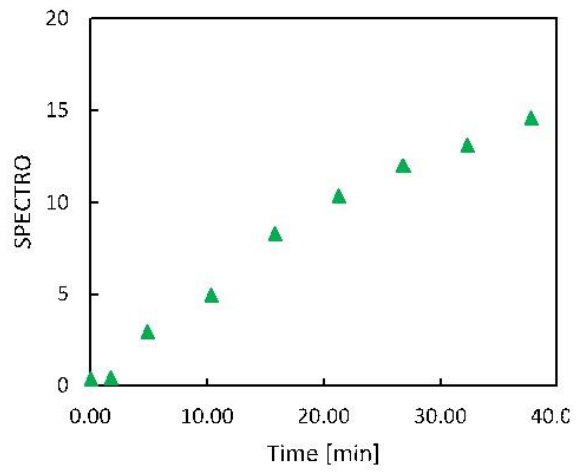
(a)



(b)

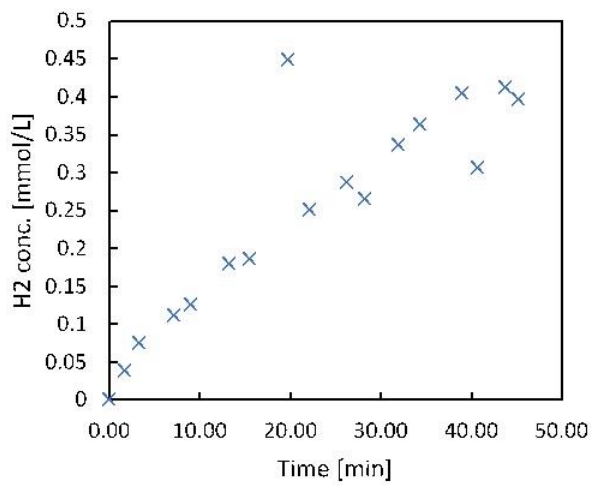


(c)

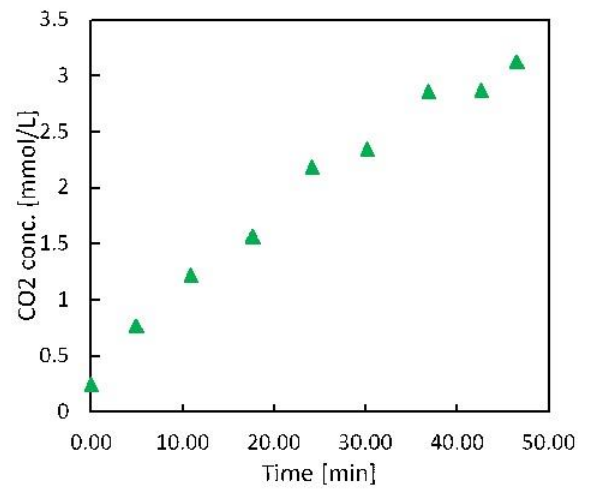


(d)

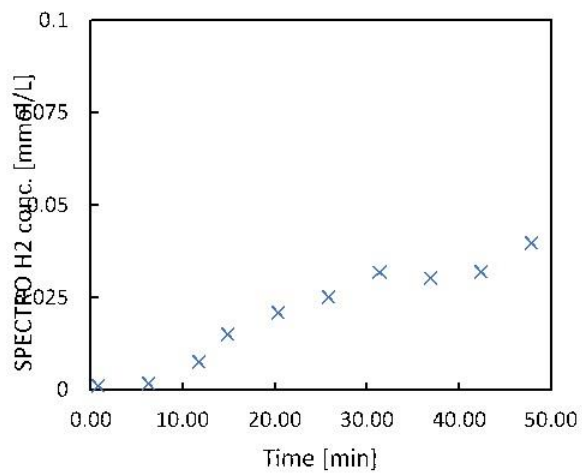
Figure 36 (a) H<sub>2</sub> and (b) CO<sub>2</sub> concentration determined by GC-method during gas sparging time in Experiment A.2 (stirring speed 60 rpm). (c) H<sub>2</sub> and (d) CO<sub>2</sub> concentration determined by SPECTRO sensor during gas sparging time in Experiment A.2 (stirring speed 60 rpm).



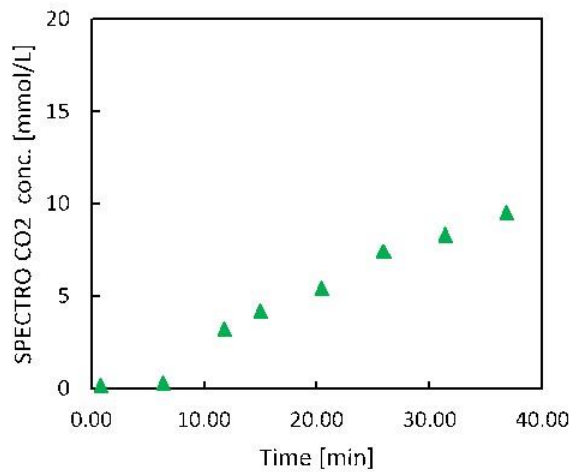
(a)



(b)

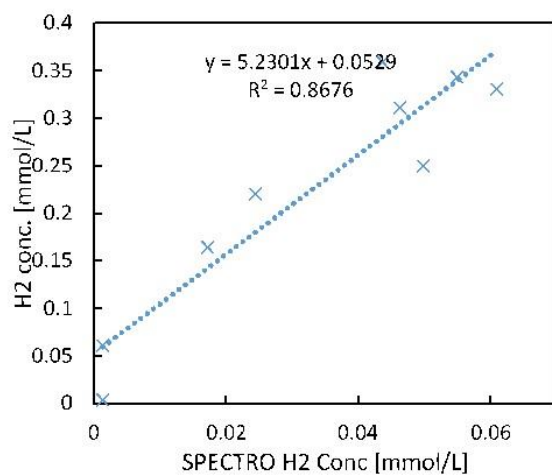


(c)

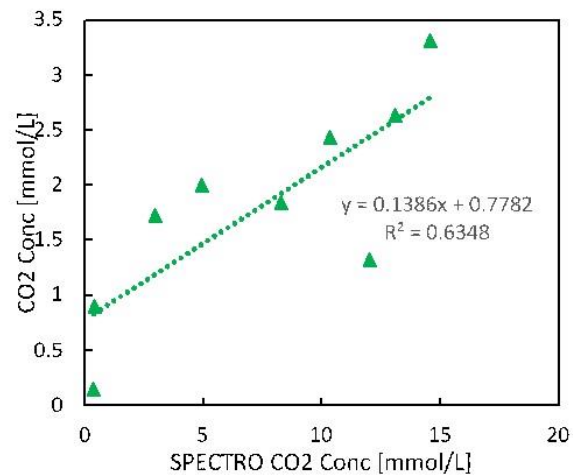


(d)

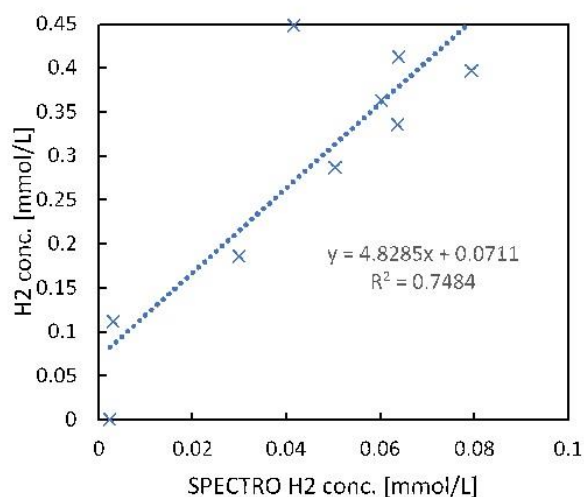
Figure 37 (a) H<sub>2</sub> and (b) CO<sub>2</sub> concentration determined by GC-method during gas sparging time in Experiment B (stirring speed 30 rpm). (c) H<sub>2</sub> and (d) CO<sub>2</sub> concentration determined by SPECTRO sensor during gas sparging time in Experiment B (stirring speed 30 rpm).



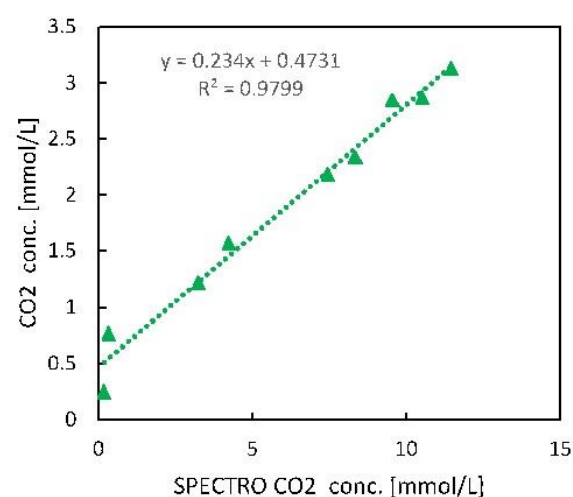
(a)



(b)



(c)



(d)

Figure 38 (a) H<sub>2</sub> and (b) CO<sub>2</sub> concentration determined by GC-method versus SPECTRO measurements in Experiment A (stirring speed 60 rpm) obtained on the same timepoints. (c) H<sub>2</sub> and (d) CO<sub>2</sub> concentration determined by GC-method versus SPECTRO measurement in Experiment B (stirring speed 30 rpm) obtained on the same timepoints.

As shown in figures 35a, 36a, and 37a after 20 minutes of gas sparging, the hydrogen concentration tends to stabilize and fluctuate around values on the same order of magnitude, and relatively close (with a maximal discrepancy of 30%) to the saturation concentration theoretically reachable ( $0.29 \text{ mmol L}^{-1}$ ) according to the Henry law and the experimental conditions chosen (i.e., hydrogen partial pressure and reactor temperature) (Grimalt-Alemany

et al., 2020, NIST 2023) . Furthermore, the gas-liquid mass transfer parameter (k<sub>la</sub>) for H<sub>2</sub> and CO<sub>2</sub> calculated using the approach followed by Grimalt-Alemaný et al. (2020) are on the same order of magnitude of values reported in the literature (Grimalt-Alemaný et al., 2020; Lovato et al., 2017). Thus, the GC-method can be regarded as reliable. In turn, the measurements obtained with the SPECTRO sensor showed high discrepancy with the measurements obtained by the GC-method (see Figure 38). The discrepancy of measurements of the hydrogen concentration was especially high, i.e., 10<sup>1</sup> (see Figures 36a, 36c; Figures 37a, 37c). On the other hand, the CO<sub>2</sub> concentration measurements obtained with the GC-method and the SPECTRO sensor were on the same order of magnitude but still in high disagreement with each other (see Figures 36b, 36d; Figures 37b, 37d; Figures 38b, 38d). However, the trends of the measured concentrations with the two methods follow similar patterns for both test species, indicating that the cause of the wrong measurements provided by the SPECTRO sensor can be miss-calibration of the sensor.

## **8. Operation of the reactor equipped with SPECTRO sensor for Anaerobic Digestion process**

The CSTR describe in sections 3 and 5 was also used to carry out continuous anaerobic digestion process using cattle manure and test the accuracy of the SPECTRO sensor in measuring the concentration of dissolved CH<sub>4</sub>, CO<sub>2</sub> and H<sub>2</sub>.

### **8.1. Methods and material**

#### **8.1.1. Substrate preparation and inoculum**

Mesophilic inoculum was supplied from digestate of a full-scale reactor located in Hashøj biogas plant (Zealand, Denmark). The cattle manure as the main substrate was also supplied from Hashøj biogas plant. Cattle manure was sieved (pore size of 4 mm) and diluted with distilled water (4% VS) to prevent clogging in the reactor tubes. After sieving and dilution, the substrate was stored at -20 °C before usage. Prior to use, the digestate was degassed by incubating at mesophilic condition for 10 days to reduce the background biogas production. The characteristics of inoculum and diluted substrates used in the experiments are presented in Table 13.

Table 13. Characteristics of substrates (after dilution) and inoculum

Characteristics	Cattle manure	Inoculum
pH	7.72	8.50
TS, g kg <sup>-1</sup>	0.054± 0.000	0.0277 ± 0.0000
VS, g kg <sup>-1</sup>	0.04 ± 0.00	0.0168 ± 0.0001

### 8.1.2. CSTR set-up

The experimental set up consisted of a continuously stirred tank reactor (CSTR) with 9.0 L total and 7.5 L working volumes operated at mesophilic condition ( $37 \pm 1$  °C). The initial HRT of the digester for start-up was considered 30 days and was decreased to 20 days after 6 days operation. An automated displacement gas metering system with a 100 mL reversible cycle and registration was used to measure biogas production rate. A peristaltic pump was used to feed the reactor every 8 h. The reactor was mixed in continuous mode at 35 rpm. The reactor stirrer is programmed through an Arduino microcontroller (Arduino Mega 2560 board). The setup was equipped with Spectro sensor together with a PC to monitor collect/record the dissolved gases involved in AD process. Moreover, a control algorithm was programmed in LabVIEW2016 software (National Instruments, Austin, TX, USA) to change the manipulated variable (i.e. feed flow rate) based on the control strategy described in section 1.1. The final experimental set-up fed with cattle manure for biogas production is shown in Figure 39. Biogas production was measured online, while VFAs concentrations were measured offline once per day. The VFAs concentrations (acetic acid, propionic acid, butyric acid, iso-butyric acid and valeric acid) were measured using an Agilent 7890A gas chromatograph (Agilent Technologies, US) equipped with a flame ionization detector (FID) and SGE capillary column (30 m length, 0.53 mm inner diameter, film thickness 1.00  $\mu$ m) with helium as carrier gas. pH trend was monitored using FiveEasy Plus Benchtop FP20 (Mettler Toledo, CH). Biogas composition was measured offline once per day with GC described in section 2.2.1.



Figure 39 The final experimental set-up fed with cattle manure for biogas production.

## 8.2. Results of reactor operation for biogas production

### 8.2.1. Start-up of the bioreactor

The digester was fed with cattle manure (4% VS). The initial HRT was set to 30 days for 6 days then was kept to 20 days as the typical HRT for stable operation of anaerobic digestion under Mesophilic condition is in the range of 15 to 25 days (Ahring et al., 2001b; Nasir et al., 2012) As shown in Figure 40 the methane production rate increased from around 200 up to 2000 mL-CH<sub>4</sub> day<sup>-1</sup>.

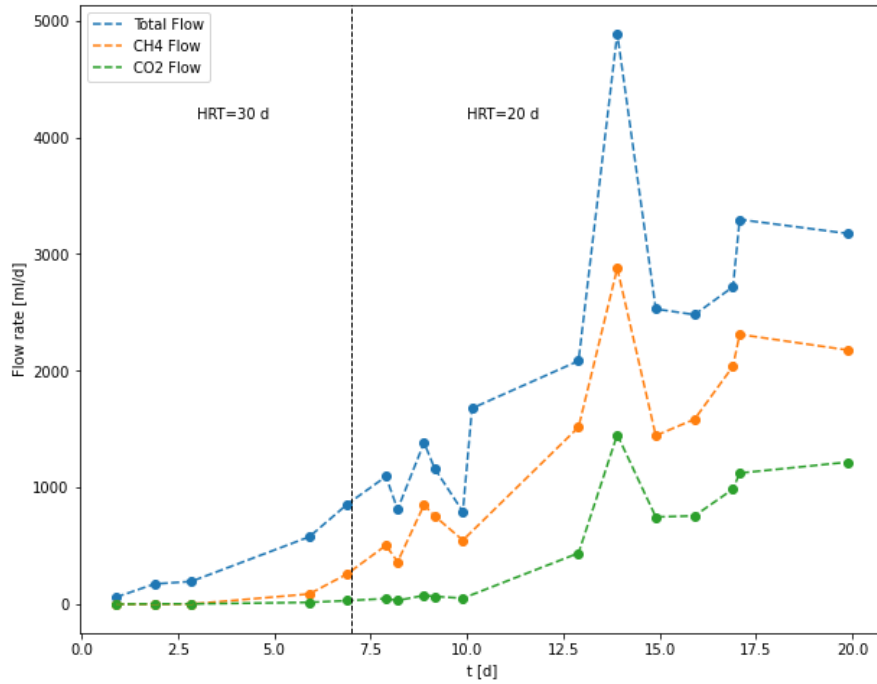


Figure 40 Methane production rate mL-CH<sub>4</sub> day<sup>-1</sup>

It should be mentioned that the control strategy was off as it was based on online VFAs concentrations (acetic acid + propionic acid) and the VFAs were measured offline with GC which was time consuming to have the data ready. The organic loading rate (OLR) was set to 1.33 and increased to 2 g VS L<sup>-1</sup> day<sup>-1</sup> which was in accordance with recommended OLR range (2–3 g VS L<sup>-1</sup> day<sup>-1</sup>) for stable operation (Ahring et al., 2001a). The pH values stabilized after 10 days of operation to an average value of 7.55 (Figure 41), which is within suggested range for stable operation of AD process. Average methane percentage in the produced biogas during the start-up period was 70% ± 5% (Figure 42), which was in accordance with the percentage of methane in biogas reported for an efficient AD process (methane (50–70%)) (Tao et al., 2019).

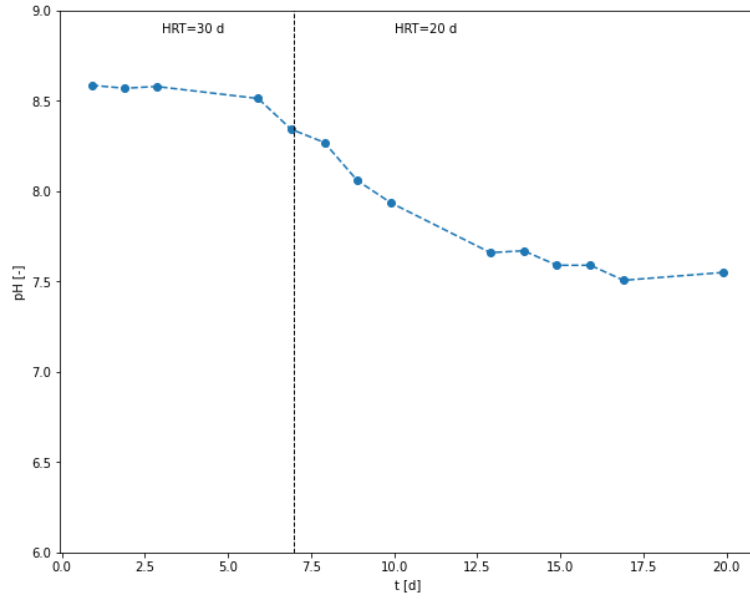


Figure 41 pH in the CSTR equipped with SPECTRO sensor

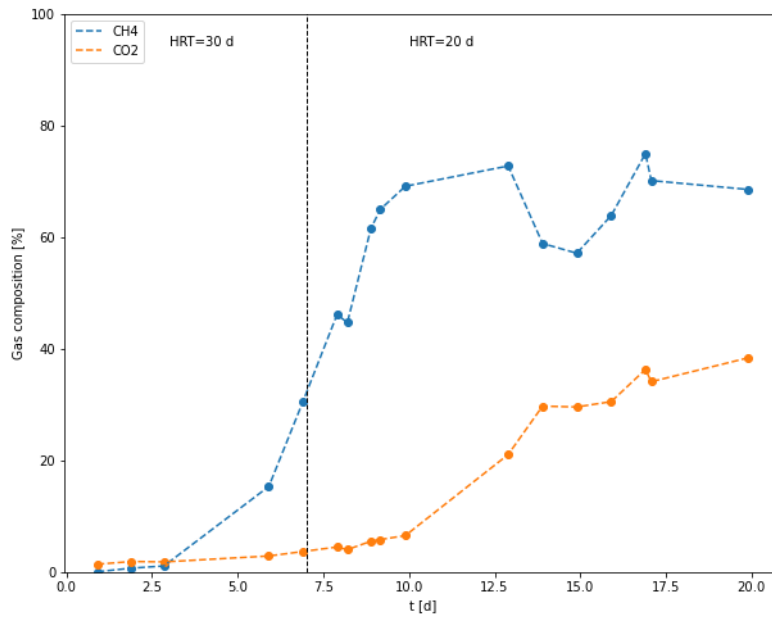


Figure 42 Biogas composition or methane percentage in %

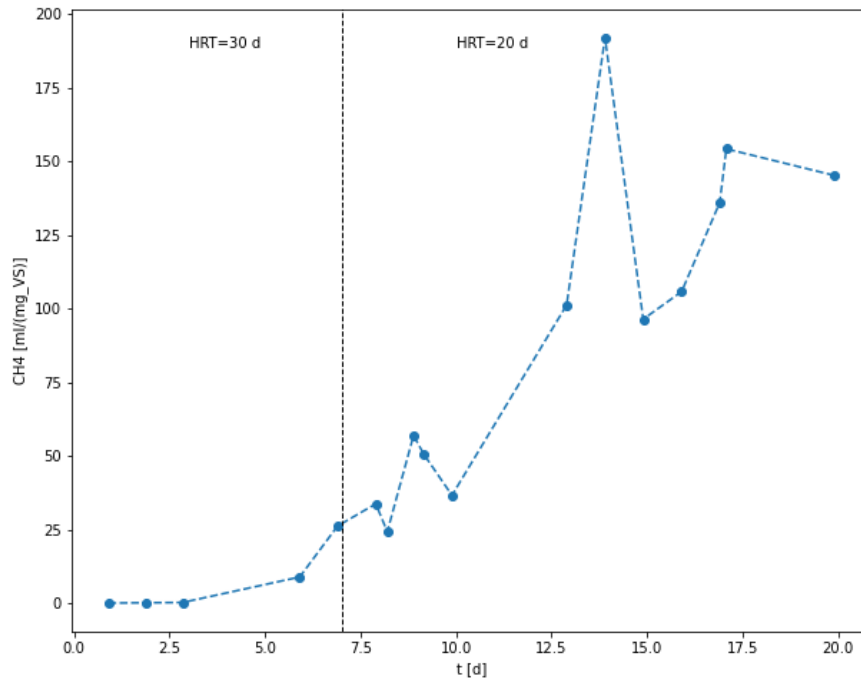


Figure 43 Methane yield (mL-CH<sub>4</sub> mg<sup>-1</sup> VS)

As it shown in Figure 43, the average methane yield after 15 days of operation was 150 mL-CH<sub>4</sub> mg<sup>-1</sup> VS.

The concentration of dissolved gases in the liquid phase such as CH<sub>4</sub>, CO<sub>2</sub>, N<sub>2</sub>, H<sub>2</sub>S, H<sub>2</sub> and NH<sub>3</sub> were measured online by SPECTRO sensor, and the results were shown in Figures 44 to 47. As it is shown, no H<sub>2</sub>S was detected by sensor during reactor operation. The dissolved CH<sub>4</sub> was increased to 0.26 mg L<sup>-1</sup> (in average) at steady state condition which is in equilibrium with the gas phase. The dissolved CO<sub>2</sub> was stabilized at 200 mg L<sup>-1</sup> after 23 days. On days 10 and 11, the reactor effluent tube was clogged for 2 hours, which led to sudden increase in dissolved gases in the liquid phase caused by over pressure in the reactor. This increase can be seen in figures 45 and 46 for concentrations of CH<sub>4</sub> and CO<sub>2</sub> in the liquid phase, respectively.

As it can be seen in Figures 44 to 47, the sensor was disconnected (shown by dashed lines in the figures) from day 13 to 14 and from day 24 for 6 days. Therefore, no data was collected during these periods.

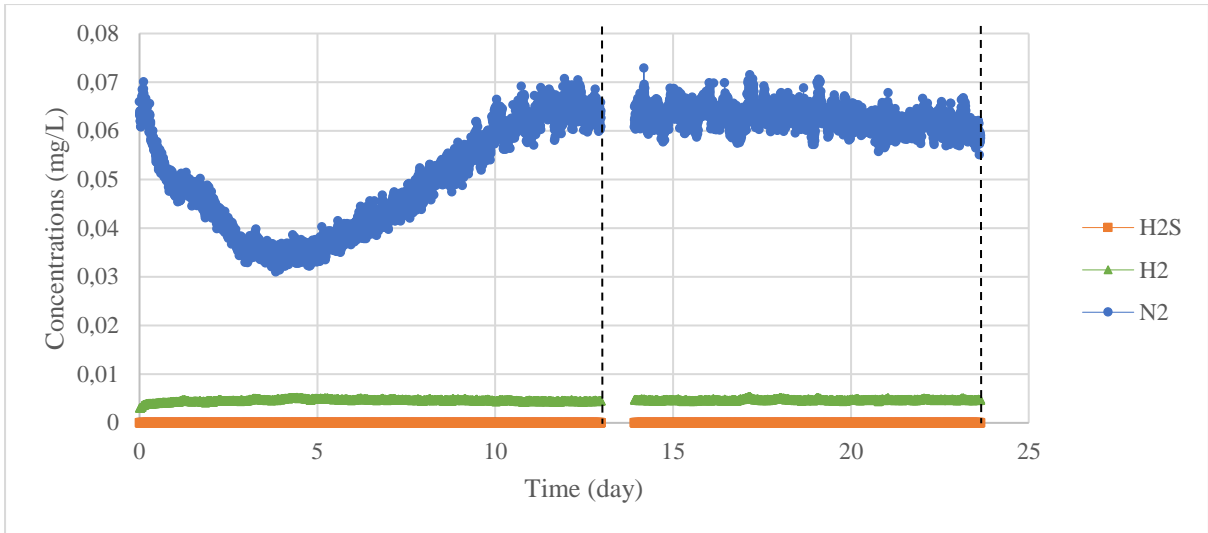


Figure 44 Concentrations of H<sub>2</sub>, N<sub>2</sub> and H<sub>2</sub>S in the liquid phase during AD operation recorded by SPECTRO sensor.

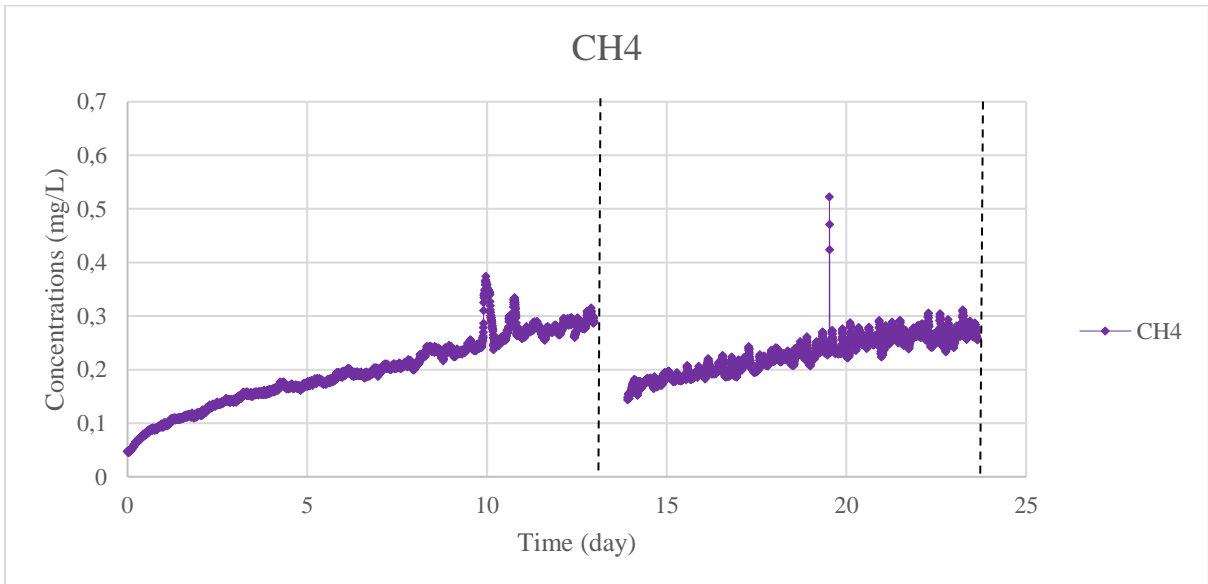


Figure 45 Concentration of CH<sub>4</sub> in the liquid phase during AD operation recorded by SPECTRO sensor.

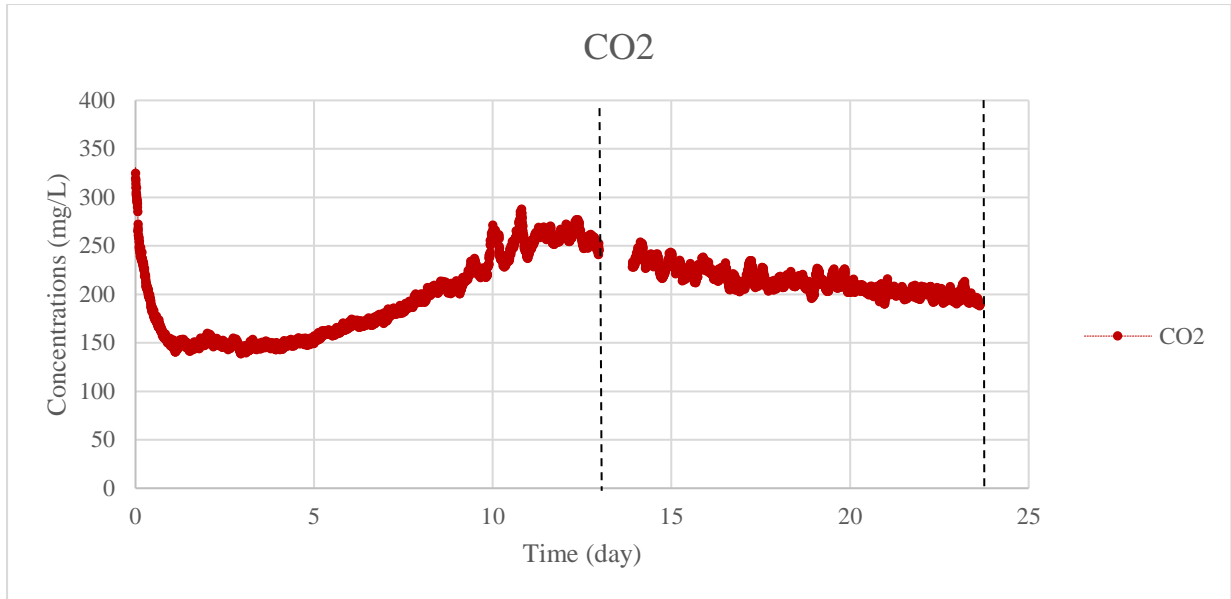


Figure 46 Concentration of CO<sub>2</sub> in the liquid phase during AD operation recorded by SPECTRO sensor.

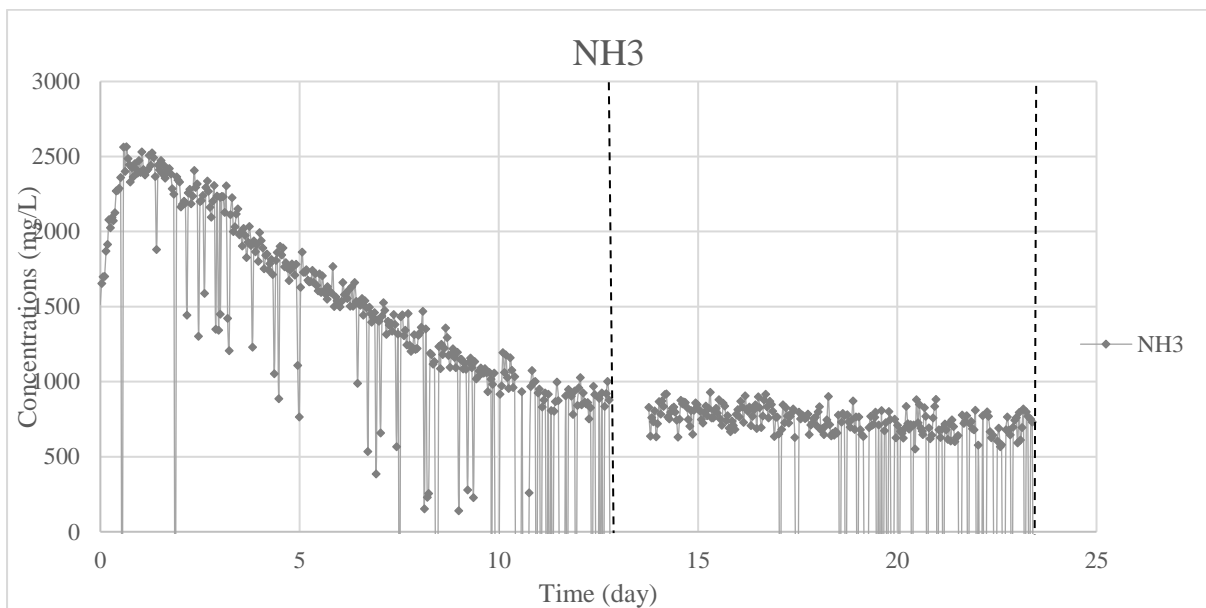


Figure 47 Concentration of NH<sub>3</sub> in the liquid phase during AD operation recorded by SPECTRO sensor.

### 8.2.2. Comparison between GC and SPECTRO measurements

As it was mentioned previously, GC measurements were conducted once per day from the reactor headspace to monitor biogas composition. The concentration of different gases in the liquid phase were calculated based on the GC measurements to validate the results recorded by SPECTRO sensor.

The calculated liquid concentration based on GC measurement was determined by means of the Henry and accounting of the partial pressures of CH<sub>4</sub> and CO<sub>2</sub> measured with the GC. The comparison between sensor results and calculated concentrations in the liquid phase (based on GC results) are shown in Figure 48. Analogously to the experiments in abiotic conditions, there is a remarkable discrepancy between the values obtained by the two methods, even though the trends of CH<sub>4</sub> and CO<sub>2</sub> concentrations in the liquid phase (after day 13, when the gas composition stabilizes) are similar. Therefore, the sensor should be re-calibrated to increase the accuracy of mass-spectroscopy method in measuring dissolved gases in the liquid phase.

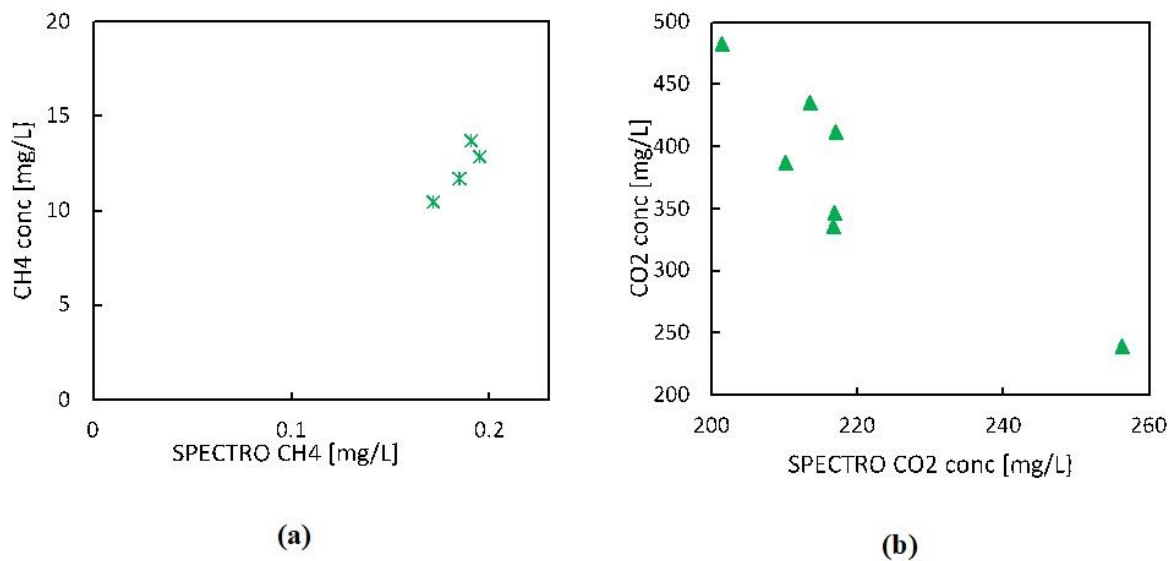


Figure 48 (a) CH<sub>4</sub> and (b) CO<sub>2</sub> concentration determined by means of the Henry law accounting of the gas composition measured with the GC versus SPECTRO measurements between day 13 and 20.

### 8.2.3. Reactor operation under co-digestion condition

The reactor will be operated for two HRTs (40 days) under the same condition feeding with 4% VS cattle manure to reach steady state condition. Afterwards the reactor performance is going to be checked with co-digestion process. Different ratios of co-digestion (at least two ratios) will be tested to select optimum co-digestion ratio for maximum methane production.

It should be noted that the results of CSRT operation equipped with SPECTRO sensor will be published in one or two high impact factor journals.

## 9. Conclusion of the DTU tests:

In this project, the performance of SPECTRO sensor developed based on mass-spectroscopy method was evaluated under abiotic and biotic conditions with the intention to use it for

monitoring of biogas plants. Different gases including CH<sub>4</sub>, CO<sub>2</sub>, H<sub>2</sub> and N<sub>2</sub> (pure and in mixture) were tested to verify the accuracy of SPECTRO sensor. By comparing the recorded data by sensor and expected results calculated based on GC results, it is clear that the SPECTRO sensor could monitor different gas concentrations in the liquid phase. However, the accuracy of the sensor was medium and needed re-calibration to increase accuracy. The SPECTRO sensor was also tested in real anaerobic digestion process for biogas production from cattle manure. Although the concentration of involved gases in AD process could be measured in the reactor liquid phase but these measurements cannot be used for process control especially for manure-based biogas digesters. Methane production rate and pH are often the online measurements monitored in industrial biogas plants. However, due to the inherent buffer capacity of feedstocks such as cattle manure, pH becomes less sensitive to process imbalances. VFAs are formed as intermediates in acidogenesis and acetogenesis steps of the AD process and therefore VFAs concentration is a more reliable indicator and can be used as a suitable controlled variable. Therefore, VFAs concentration together with methane production rate would be ideal indicators for process monitoring and control. Unfortunately, SPECTRO sensor was not able to measure VFAs, which are considered the most reliable indicators for online monitoring and control of AD process and the reactor operation was conducted without activation of control algorithm. Although, the performance of a previous control strategy like suggested control strategy in this project was tested in our group at DTU. This control strategy was based on total VFAs concentration measured by manual titration method. The previous experimental results confirmed that the total VFAs concentration, as an additional measurement, could improve the performance of the reactor control system especially for systems with high buffer capacity (treating manure). The suggested control strategy could successfully improve the methane production rate and keep the reactor stable against external severe disturbances. Conclusively, a control strategy based on online titrimetric methods for VFAs measurements together with online monitoring of methane production can be considered as ideal for development of future monitoring and control technology of biogas process.

## **10. General discussion and economic perspectives.**

From the DTU trials it is established that the sensor is not able to measure VFAs, and can as such not be considered optimal for process monitoring and control. However, it can measure several other dissolved gasses in the liquid phase of a digester, which are of considerable interest for the operation of the plant, namely CH<sub>4</sub>, CO<sub>2</sub>, NH<sub>3</sub> and H<sub>2</sub>S. The CH<sub>4</sub>/CO<sub>2</sub> ratio

is decisive for the energy value of the biogas produced, and the plant manager would normally be interested in as high a CH<sub>4</sub>/CO<sub>2</sub> ratio as possible. Not only is the very ratio of considerable interest, but also changes in it may lead to the need for operational changes. The ratio can be influenced by the composition of the substrates applied to the plant. If the ratio is too low, or declining, it is an indication that additional substrates with higher fat contents might be favorable to apply to increase the CH<sub>4</sub> ratio of the biogas produced.

In addition, H<sub>2</sub>S and NH<sub>3</sub> at certain levels involve danger of inhibiting the methanisation process in the digester. Especially NH<sub>3</sub> inhibition is linked to Ph levels, but if Ph is not measured on-line, but must be made manually, on-line measuring of NH<sub>3</sub> is a very good indicator for the inhibition danger. But of course, the plant manager needs to know exactly where the tipping point is, at which NH<sub>3</sub> level inhibition occurs, which can be established in lab scale trials. Again, not only the very level of NH<sub>3</sub> is of interest, but also changes are valuable knowledge, as they indicate if changes in the substrate composition is required to avoid inhibition. The same arguments are true for H<sub>2</sub>S.

Finally, the sensor can measure CH<sub>4</sub> dissolved in the liquid phase. Changes in the CH<sub>4</sub> content indicates whether the process is deteriorating or recovering and improving its performance. Changes will immediately show by the gas measurement equipment of the plant, so this feature of the sensor is less important.

So even if the Spectro Biogas sensor system cannot be sold as the one and only optimal system for process monitoring and control, it does have measuring abilities that should not be ignored by agricultural biogas plants in Denmark. Furthermore, it is possible that agricultural plants in other countries, which apply much higher proportions of energy crops may have lower Ph levels, which allow the sensor to measure also VFAs, which would substantially increase the benefits from the system.

Even in the Danish context, the Spectro Biogas sensor may prove to be a profitable investment, as it, according to Spectro Biogas, can be installed for only 500.000 DKK, with annual operating costs of approximately 50.000 DKK. This is not a huge amount considering that it is able to monitor if NH<sub>3</sub> or H<sub>2</sub>S inhibition is under way, but also the composition of the biogas, which is always of considerable interest.

## References:

- Ahring, B. K., Ibrahim, A. A., & Mladenovska, Z. (2001a). Effect of temperature increase from 55 to 65°C on performance and microbial population dynamics of an anaerobic reactor treating cattle manure. *Water Research*, *35*(10), 2446–2452. [https://doi.org/10.1016/S0043-1354\(00\)00526-1](https://doi.org/10.1016/S0043-1354(00)00526-1)
- Ahring, B. K., Ibrahim, A. A., & Mladenovska, Z. (2001b). EFFECT OF TEMPERATURE INCREASE FROM 55 TO 65°C ON PERFORMANCE AND MICROBIAL POPULATION DYNAMICS OF AN ANAEROBIC REACTOR TREATING CATTLE MANURE. *Wat. Res*, *35*(10), 2446–2452.
- Ahring, B. K., Sandberg, M., & Angelidaki, I. (1995). Volatile fatty acids as indicators of process imbalance in anaerobic digestors. *Applied Microbiology and Biotechnology*, *43*(3), 559–565. <https://doi.org/10.1007/BF00218466/METRICS>
- Boe, K., & Angelidaki, I. (2006). *Online monitoring and control of the biogas process*.
- Boe, K., Batstone, D. J., Steyer, J. P., & Angelidaki, I. (2010). State indicators for monitoring the anaerobic digestion process. *Water Research*, *44*(20), 5973–5980. <https://doi.org/10.1016/J.WATRES.2010.07.043>
- Chen, Y., Cheng, J. J., & Creamer, K. S. (2008). Inhibition of anaerobic digestion process: A review. *Bioresour Technol*, *99*(10), 4044–4064. <https://doi.org/10.1016/J.BIORTECH.2007.01.057>
- Grimalt-Alemany, A., Asimakopoulou, K., Skiadas, I. V., & Gavala, H. N. (2020). Modeling of syngas biomethanation and catabolic route control in mesophilic and thermophilic mixed microbial consortia. *Applied Energy*, *262*. <https://doi.org/10.1016/J.APENERGY.2020.114502>
- Jacobi, H. F., Moschner, C. R., & Hartung, E. (2009). Use of near infrared spectroscopy in monitoring of volatile fatty acids in anaerobic digestion. *Water Science and Technology*, *60*(2), 339–346. <https://doi.org/10.2166/WST.2009.345>
- Jimenez, J., Latrille, E., Harmand, J., Robles, A., Ferrer, J., Gaida, D., Wolf, C., Mairet, F., Bernard, O., Alcaraz-Gonzalez, V., Mendez-Acosta, H., Zitomer, D., Totzke, D., Spanjers, H., Jacobi, F., Guwy, A., Dinsdale, R., Premier, G., Mazhegrane, S., ... Steyer, J. P. (2015). Instrumentation and control of anaerobic digestion processes: a review and some research challenges. *Reviews in Environmental Science and Bio/Technology 2015 14:4*, *14*(4), 615–648. <https://doi.org/10.1007/S11157-015-9382-6>
- Lackner, N., Wagner, A. O., & Illmer, P. (2020). Effect of sulfate addition on carbon flow and microbial community composition during thermophilic digestion of cellulose. *Applied Microbiology and Biotechnology*, *104*(10), 4605–4615.
- Lovato, G., Alvarado-Morales, M., Kovalovszki, A., Peprah, M., Kougiyas, P. G., Rodrigues, J. A. D., & Angelidaki, I. (2017). In-situ biogas upgrading process: Modeling and simulations aspects. *Bioresour Technol*, *245*, 332–341. <https://doi.org/10.1016/j.biortech.2017.08.181>
- Molina, F., Castellano, M., García, C., Roca, E., & Lema, J. M. (2009). Selection of variables for on-line monitoring, diagnosis, and control of anaerobic digestion processes. *Water Science and Technology*, *60*(3), 615–622. <https://doi.org/10.2166/WST.2009.379>

- Nasir, I. M., Mohd Ghazi, T. I., & Omar, R. (2012). Anaerobic digestion technology in livestock manure treatment for biogas production: A review. *Engineering in Life Sciences*, *12*(3), 258–269. <https://doi.org/10.1002/ELSC.201100150>
- Nguyen, D., Gadhamshetty, V., Nitayavardhana, S., & Khanal, S. K. (2015). Automatic process control in anaerobic digestion technology: A critical review. *Bioresource Technology*, *193*, 513–522. <https://doi.org/10.1016/J.BIORTECH.2015.06.080>
- Petre, E., Selişteanu, D., & Şendrescu, D. (2013). Adaptive and robust-adaptive control strategies for anaerobic wastewater treatment bioprocesses. *Chemical Engineering Journal*, *217*, 363–378. <https://doi.org/10.1016/J.CEJ.2012.11.129>
- Peu, P., Picard, S., Diara, A., Girault, R., Béline, F., Bridoux, G., & Dabert, P. (2012). Prediction of hydrogen sulphide production during anaerobic digestion of organic substrates. *Bioresource Technology*, *121*, 419–424.
- Process Dynamics and Control - Dale E. Seborg, Thomas F. Edgar, Duncan A. Mellichamp, Francis J. Doyle, III - Google Books.* (n.d.). Retrieved August 3, 2023, from [https://books.google.dk/books?hl=en&lr=&id=ZZVFEEAAQBAJ&oi=fnd&pg=PA1&ots=qN9o87DPGR&sig=EpBaUZeAsboJppZqtPIiiv6UMc&redir\\_esc=y#v=onepage&q&f=false](https://books.google.dk/books?hl=en&lr=&id=ZZVFEEAAQBAJ&oi=fnd&pg=PA1&ots=qN9o87DPGR&sig=EpBaUZeAsboJppZqtPIiiv6UMc&redir_esc=y#v=onepage&q&f=false)
- Steyer, J. P., Buffière, P., Rolland, D., & Moletta, R. (1999). Advanced control of anaerobic digestion processes through disturbances monitoring. *Water Research*, *33*(9), 2059–2068. [https://doi.org/10.1016/S0043-1354\(98\)00430-8](https://doi.org/10.1016/S0043-1354(98)00430-8)
- Tao, Y., Evren Ersahin, M., Ghasimi, D. S. M., Ozgun, H., Wang, H., Zhang, X., Guo, M., Yang, Y., Stuckey, D. C., & Van Lier, J. B. (2019). *Biogas productivity of anaerobic digestion process is governed by a core bacterial microbiota.* <https://doi.org/10.1016/j.cej.2019.122425>
- Weiland, P. (2010). Biogas production: Current state and perspectives. *Applied Microbiology and Biotechnology*, *85*(4), 849–860. <https://doi.org/10.1007/S00253-009-2246-7/FIGURES/4>